Role of Polymer–Particle Adhesion in the Reinforcement of Hybrid Hydrogels

Anne-Charlotte Le Gulluche, Nadège Pantoustier, Annie Brûlet, Olivier Sanseau, Paul Sotta, Alba Marcellan

The role of polymer-particle adhesion in the reinforcement of hybrid hydrogels

Anne-Charlotte Le Gulluche,[†,‡] Nadège Pantoustier,[¶,‡] Annie Brûlet,[¶] Olivier Sanseau,[§] Paul Sotta,[*,†,‖] and Alba Marcellan[*,‡,⊥]

†*Laboratoire Polymères et Matériaux Avancés, UMR5268, CNRS, Solvay, 69192 Saint Fons cedex, France*

‡*Sciences et Ingénierie de la Matière Molle, UMR7615, ESPCI Paris, PSL University, Sorbonne Université, CNRS, F-75005 Paris, France*

¶*Laboratoire Léon Brillouin, UMR12, CEA, CNRS, Université Paris Saclay, C. E. Saclay, 91 191 Gif Sur Yvette cedex, France*

§*Solvay R&I PM2D, 69192 Saint Fons Cedex, France*

‖*Ingénierie des Matériaux Polymères, UMR 5223, Université de Lyon, CNRS, Université Lyon 1, INSA Lyon, UJM, 69621 Villeurbanne cedex, France*

⊥*Institut Universitaire de France*

E-mail: paul.sotta@insa-lyon.fr; alba.marcellan@espci.psl.eu

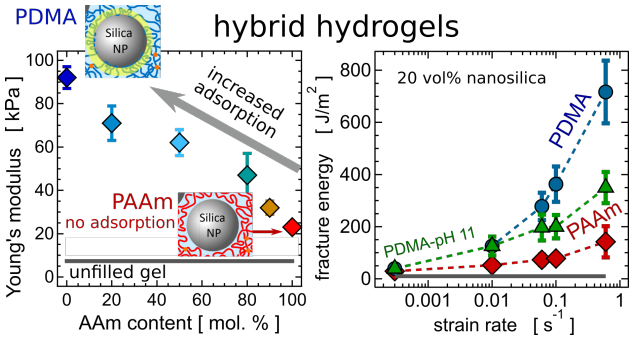

For Table of Contents use only

Abstract

Model hybrid hydrogels reinforced by silica nanoparticles were carefully designed to selectively tune the polymer-particle interactions while maintaining similar dispersion states of the nanoparticles. This was achieved by changing the nature of the polymer in the gel matrix from poly(dimethylacrylamide) (PDMA), which adsorbs on silica in aqueous suspension, to red poly(acrylamide) (PAAm), which does not, and by polymerizing and cross-linking the gels in-situ. The adsorption on silica of both polymers was first quantified by considering linear chains of PDMA or PAAm or random copolymers of both. Changing the pH may also inhibit PDMA adsorption on silica. The properties of gels of PDMA, PAAm and co-polymers were then characterized. The specific effect of polymer adsorption on mechanical properties was demonstrated, other parameters, specifically the dispersion state of silica, being kept roughly constant. The Young's modulus, or equivalently the reinforcement in the linear regime, depends monotonically on the fraction of dimethylacrylamide monomers in the gel. It is enhanced by a factor of 5 due to adsorption only. Adsorption, which is a dynamic process, enhances the dependence of the fracture energy G_c on the draw rate. While G_c is little increased at low draw rate, it is increased by one order of magnitude at high draw rate with respect to the value in the same gel built with non-adsorbing monomers.

1 Introduction

The hybridization between hydrogel networks and inorganic nanoparticles has been proposed first in 2002 by Haraguchi who designed hydrogels with poly(N-alkylacrylamide) filled with clay nanosheets.[1] Since then, the research on nanocomposite gels has remained very active[2–5]. Following the work of Lafuma et al. on semi-dilute solutions,[6] our group has developped model gels by *in situ* polymerization of a polymer network in the presence of silica aqueous solutions.

Introducing silica nanoparticles in a polymer matrix to form hybrid gels induces out-

standing mechanical properties.[7–9] Remarkably, both the elastic modulus and the elongation at break can be drastically increased, eventually leading to an enhancement of the energy at break or gel toughness by several decades. The fracture toughness or resistance to crack propagation may also be drastically enhanced.[10] These results have paved the way for a new gluing method for gels and biological tissues using solid suspensions of nanoparticles as adhesive.[11] Reported studies on PDMA/silica hybrid gels clearly indicate that polymer adsorption is key for gel toughening or adhesion properties.[11–13] In poly(acrylamide) gels, polymer/silica adsorption was tuned by using aluminium-modified silica nanoparticles.[14]

Viscoelastic properties of nanocomposite gels have been extensively studied but only few studies were carried out to understand and quantify the interactions at the solid/liquid interfaces.

Elucidating the relative contributions of the various physical mechanisms at play remains a key challenge, though. In this paper, the impact of polymer adsorption on hydrogel toughening is studied by tuning the reversible polymer/silica interactions. Two experimental strategies were designed in order to control and tune the strength of polymer adsorption onto silica nanoparticles regardless of the gel structure, by synthetizing series of model gels.

In the first series of model gels, the nature of the monomer was changed from N,N-dimethylacrylamide (DMA), which interacts with silica, to acrylamide (AAm), which does not (see figure 1), while keeping constant other key parameters such as the surface chemistry and the dispersion state of the silica nanoparticles. As published studies report conflicting results, with some authors argueing on the presence of strong interactions between PAAm and silica,[15] the first step of this study was to assess that AAm does not adsorb onto silica, in contrast to DMA.[16]

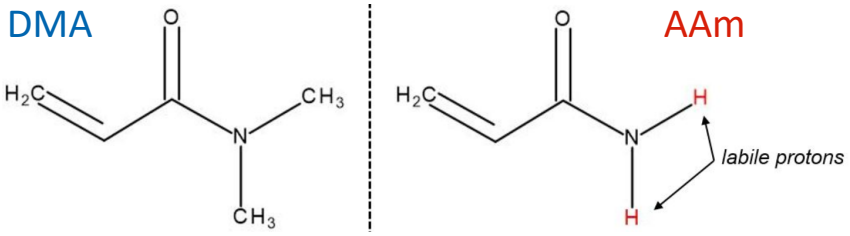

Figure 1: Left: N,N-dimethylacrylamide (DMA) and Right: acrylamide (AAm) monomers.

Some attempts to synthesize PAAm/silica nanocomposites hydrogels have been already published, with some of them showing a decrease of mechanical properties using PAAm as compared to PDMA gels, but the swelling state was not precisely controlled.[7,13] It was confirmed that silica nanoparticles embedded in PDMA matrix are well-dispersed.[8] However, it has not been checked yet that the same dispersion state can be obtained in PAAm/silica hybrid gels, so that the impact of reversible interactions alone can be evaluated. It is therefore essential to thoroughly investigate the structure and behavior of PDMA and PAAm hybrid gels of similar structures while keeping control over the chemical environment of the nanoparticles (pH, ionic force, dispersion state) so as to discriminate the role of polymer adsorption.

In a second series of gels, polymer/nanoparticles interactions were disturbed by tuning the surface chemistry of the nanoparticles. Polymer adsorption is very sensitive to experimental conditions. Experimental evidences point out that it occurs within a certain range of parameter values in term of polymer/solvent and polymer/substrate affinities, nanoparticle nature and chemical environment (pH and ionic force).[17,18] This is also supported by theoretical works.[19–21]

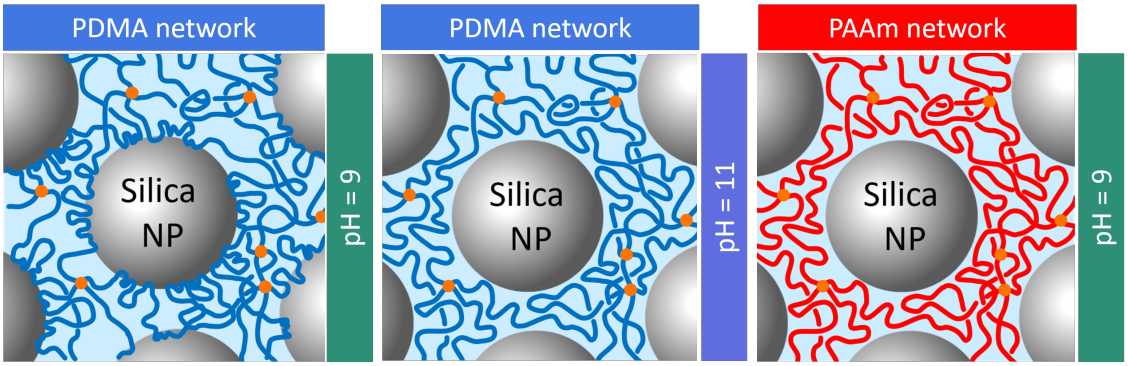

Figure 2: Left, schematics of a PDMA/silica hybrid hydrogel synthetized at pH = 9, combining covalent cross-links (orange dots) and physical interactions (polymer chains adsorbed at the surface of silica nanoparticles). Middle, PDMA hybrid hydrogel synthetized at pH = 11, in which polymer adsorption is inhibited. Right, PAAm hybrid gel, in which polymer chains do not interact with silica NPs.

The general architecture of hybrid hydrogels is schematized in figure 2. The compositions of the hybrid gels were set to reach a compromise between stretchability and stiffness. Three important points should be underlined: (1) a small amount (0.1 mol%) of chemical cross-linker was added to control the network topology. This value is a compromise to overcome the ill-controlled self cross-linking that may take place during polymerization[22] and to avoid dramatic reduction of the extensibility; (2) all gels were characterized in the preparation state, with a well-controlled matrix hydration and a fixed silica volume fraction 20 vol%; (3) A specific synthesis route was developed for PAAm/silica hybrid gels in order to keep good control of the dispersion state of silica nanoparticles.

The use of NMR spectroscopy for the characterization of polymer hydrogels and organogels is a growing field[23–27]. Time-domain proton NMR is used here for two distinct purposes. First, measuring proton relaxation functions provides direct determination of the immobilized (adsorbed) polymer fraction at the interface with the silica nanoparticles. Secondly, multiple-quantum (MQ) proton NMR gives insight into the structure of the gel network, namely the cross-linking and/or entanglement density, homogeneity of the gel network and the fraction of non-elastic chains in the networks (the so-called network defects), i.e. the sol fraction and/or unreacted chains and oligomers, dangling chains and close loops.

In the first part of the paper, the differences in adsorption of PDMA and PAAm on silica are quantified in linear polymers. As a first step, we show sorption isotherms of PDMA, PAAm and random copolymers of both co-monomers on silica nanoparticles in aqueous solution. We then shift to hybrid hydrogels of PDMA, PAAm and copolymers filled containing 0.1 mol% cross-linkers and the same silica nanoparticles. The good dispersion state of silica nanoparticles in both hydrogels is assessed. We quantify the adsorption and show that the adsorbed amounts are comparable to those measured with the corresponding linear polymer chains, which means that crosslinking does not significantly preclude adsorption.

We then show the effect of adsorption on the linear viscoelastic modulus and on the apparent crosslink density (as measured by NMR). We further illustrate the impact of adsorption on the fracture properties of the hybrid gels.

The paper is organized as follows. The studied materials, synthesis procedure and experimental techniques are described in Section 2 for both linear polymers and hydrogels. Sorption isotherms of linear polymer chains are presented in Section 3.1. Results on polymer adsorption in hybrid hydrogels, as measured by Proton NMR relaxometry, are presented in Section 3.2. The effects of changing the nature of the monomer and the pH are discussed. The characterization of the structure of the hybrid hydrogel networks by DQ proton NMR is presented in Section 3.3. The impact of the polymer/particle interactions on mechanical and fracture properties is then discussed in Section 3.4.2.

2 Materials and methods

2.1 Synthesis and preparation of polymers and gels

Ludox TM-50 silica nanoparticle solutions were bought from Sigma-Aldrich and used without further purification. The nanoparticles were characterized by SEM and Small Angle X-Ray scattering (SAXS). SAXS data fitted for polydisperse spherical particles with a Gaussian size distribution give a mean radius of 13.5 nm with a standard deviation $\sigma = 0.13$. The

corresponding surface area is 100 m^2/g, considering a specific weight of 2.3 g/cm^3.

Silica aqueous solutions were deuterated for the purpose of NMR measurements. Pure Ludox TM-50 was dialyzed against D_2O using a dialysis membrane with cut-off 6-8 kDa purchased from Sigma-Aldrich and used after 30 minutes rinse in D_2O. Dialysis solvent was changed every 5 days, this step was repeated three times to ensure proper deuteration of silica. Dialyzed silica maximum concentration was evaluated at 24.85 wt%. Control DLS measurements did not show any signature of particle agglomeration.

2.1.1 Synthesis of linear chains

To get better insight on polymer adsorption in PDMA and PAAm hybrid gels, linear polymer chains targeting the average length between two cross-link points in hybrid gels cross-linked at 0.1 mol% were first synthesized. This length amounts to about 50 000 g/mol for PDMA gels. Higher chain lengths were then targeted to assess the impact of the chain size on adsorption. Linear chains of homopolymers and copolymers of poly(acrylamide) (AAm) and poly(N, N-dimethylacrylamide) (DMA) of controlled size (targeted M_n of 50 000, 200 000 and 500 000 g/mol) were synthesized using Atom Transfer Radical Polymerization (ATRP) (see the Supplementary Information (**SI**) file). The synthetized polymers PAAm-x or PDMA-x, x being the targeted M_n in kg/mol. The copolymers P(AAm-co-DMA) are denoted PAD$y/z - x$ with y and z the molar contents of AAm and DMA respectively. For example, a copolymer containing 20 mol% of AAm and 80 mol% of DMA with a targeted M_n of 50 000 g/mol will be denoted PAD20/80-50. The synthetized polymer chains were characterized by Size Exclusion Chromatography (SEC). The synthesized homopolymers and copolymers with different targeted M_n are summarized in Table 1.

Table 1: The list of synthesized linear polymers. The number average molecular mass M_n and dispersity D were determined by SEC. The targeted molar masses M_n^{target} are also indicated. * indicate syntheses in which the obtained M_n values are larger than targeted ones, which points to a loss of control of the polymerization (see also Table 2 in **SI**).

Polymer	M_n (g/mol)	M_n^{target} (g/mol)	D
PAAm-50	68 000	50 000	1.3
PDMA-50	63 000	50 000	1.5
PAD80/20-50	74 000	50 000	1.6
PAD50/50-50	150 000*	50 000	2.01
PAD20/80-50	78 000	50 000	1.7
PAAm-200	230 000	200 000	1.7
PDMA-200	155 000	200 000	1.4
PDMA-500	740 000*	500 000	1.4
PAD80/20-200	160 000	200 000	1.5
PAD50/50-500	650 000	500 000	1.4
PAD20/80-200	190 000	200 000	1.7

The ratio of AAm and DMA in the obtained copolymers were checked using ^{1}H NMR which allowed to conclude that reactivities of both monomers are quite close, thus indicating a statistical copolymerization.

For homopolymers, the target number average mar masses were approximately reached with experimental M_n of 63 000 g/mol and 68 000 g/mol for PDMA and PAAm respectively, for a targeted M_n of 50 000 g/mol. The dispersity D of the homopolymers remains of the order 1.5, which confirms the relatively good control of the polymerization. For copolymers, even though the obtained M_n values remain close to the targeted one (50 000g/mol), the dispersities are often a little higher than those of homopolymers. Reactions involving PDMA are more difficult to control due to the exothermicity of the reaction: control has certainly been lost in the synthesis of PAD-50/50-50, as both the dispersity and molar mass are much higher than expected.

The obtained dispersities are much higher than what could be expected for a perfectly successful ATRP synthesis, with D within the 1.05-1.1 range[28]. However, it is important to underline that ATRP is not the best way to conduct Controlled Radical Polymerization of acrylamide and derivatives, which is usually performed by Reversible Addition Frag-

mentation Chain Transfer (RAFT)[29–31], since difficulties in maintaining high and constant ATRP equilibrium with acrylamides were reported[32]. ATRP was selected here as it allows synthetizing both homopolymers and statistic copolymers using one single commercially available initiator for both monomers while RAFT synthesis would usually require a specific initiator for each type of monomer. Good control of both the polymer chain size and the molecular weight distribution ($D < 1.2$) in the RAFT synthesis of acrylamides using only one initiator for several types of monomers was recently reported[33]. However, the proposed path involved the synthesis of RAFT/MADIX agents, which added a supplementary synthesis step for the polymerization. Successful ATRP of poly(N-alkyl)acrylamides with good control over M_n and relatively low dispersity was reported[34]. Furthermore, Wever and *al.* reported ATRP synthesis of N-isopropylacrylamide (PNIPAm) and block copolymers of poly(NIPAm-co-AAm) in aqueous solvent at RT, which is preferable for practical, safety and environmental reasons[35].

The polymerization process relies on the equilibrium between dormant and active species and is catalyzed by the Cu/ Me_6-TREN ligand/metal complex. Me_6-TREN is an hindered tetradentate ligand bearing four nitrogen groups dedicated to complexing the copper atom. Poly(N-alkylacrylamides) and poly(acrylamide) also contain a large amount of nitrogen atoms. The catalyzer may then perhaps be deactivated by the growing polymer chains, leading to a loss of control of the equilibrium between dormant and active species, which would lead to Free (not Controllled) Radical Polymerization. Exothermicity may also lead to a loss of control, as radical may be generated more rapidly.

2.1.2 Synthesis of gels

Hybrid hydrogels based on PDMA, PAAm and copolymers were prepared at controlled pH by *in situ* free radical polymerization, using N, N'-methylenebisacrylamide (MBA) as the cross-linker and potassium persulfate (KPS)/N, N, N', N'-tetramethylethylenediamine (TEMED) as redox initiators (see **SI**).

As in both cases polymerization takes place via a radicalar process, the polymer structure should be identical to that of linear chains. ATRP makes it possible to control the molar mass and to obtain low dispersity to better understand adsorption phenomena. When synthesizing hydrogels, polymerization does not need to be controlled because polymer chains are cross-linked, so they can be obtained by free radical polymerization, which is simpler to implement. Besides, in ATRP, the presence of a copper-based catalyst in the network would make purification more complex.

Two distinct series of hybrid hydrogels were synthetized. In the first series (see Table 2), the fraction of DMA and AAm comonomers was varied while keeping constant both the silica volume fraction (20 vol%) and the cross-link density (MBA/monomer molar ratio 0.1 mol%). For all compositions, the amounts of co-initiators were fixed at m_{KPS}= 0.041 g and v_{TEMED} = 22.5 μL, and the amount of chemical cross-linker was fixed at m_{MBA}= 2.3 mg. The samples shall be denoted NC_D (PDMA gels), NC_A (PAAm gels) or NC_A_x-D_y (copolymer gels with molar fractions x and y of AAm and DMA comonomers respectively) (NC means 'Nanocomposite').

In the second series, PDMA and PAAm gels with varying silica volume fractions (0 to 10 vol%) and cross-link densities (MBA/monomer molar ratio from 0 mol% to 1 mol%) were synthetized (see Table 3). Samples shall be denoted 'A' for AAm-based gels or 'D' DMA-based gels, 'R_z', with 'z' the molar ratio of cross-linker to monomer, 'SP_x' with 'x', the silica volume fraction. As an example, a PDMA gel cross-linked at 0.1 mol% with a silica volume fraction of 10 vol% shall be denoted D_SP10_R01. Gels with modified silica surface chemistry (synthetized at pH 11) are denoted accordingly with suffix _pH11. Besides, this second series was prepared in D_2O for NMR measurements. The formulations of all studied hybrid hydrogels are summarized in Table 3. Unfilled gels (0 vol% silica, denoted *_SP0_*) shall serve as references.

Measurements were performed in the hydrogel preparation state, with a fixed polymer/D_2O molar ratio equal to 0.028 (with M_{AAm}= 71.08 g/mol and M_{DMA}= 99.13 g/mol), which cor-

responds to a matrix hydration degree 87.7 wt% or equivalently to a polymer molar fraction, $\phi_{mol} = 0.026$.

Table 2: Nomenclature of the first series of hybrid hydrogels. The molar ratios of each comonomer are indicated. SR is the swelling ratio of the gel calculated as $SR = Q_e/Q_0$, Q_e and Q_0 being respectively the measured equilibrium swelling and the theoretical initial swelling, corresponding to the preparation state and calculated according to Eqs. (2) and (3) in **SI**. The silica volume fraction (the volume ratio of silica nanoparticles to the total volume of hybrid hydrogels) is fixed at 0.2 (using $\rho_{Si} = 2.3 \times 10^6$ g.cm^{-3}) and the cross-linker/monomer ratio is 0.1 mol% (see also Table 3 in **SI**).

Nomenclature	[AAm] (mol%)	[DMA] (mol%)	Q_0	$SR = Q_{eq}/Q_0$	extractible (wt%)
NC_A	100	0	11.34	17 ± 3	1.96
NC_D	0	100	8.45	3.4 ± 0.4	1.81
NC_D_pH11	0	100			
NC_A_{99}-D_1	99	1	11.34	16.8 ± 0.4	1.51
NC_A_{90}-D_{10}	90	10	11.13	7.2 ± 0.1	1.78
NC_A_{80}-D_{20}	80	20	10.59	5.3 ± 0.4	1.03
NC_A_{50}-D_{50}	50	50	9.65	4.1 ± 0.2	0.94
NC_A_{20}-D_{80}	20	80	8.88	3.9 ± 0.3	0.87

Table 3: Nomenclature of the second series of hybrid hydrogels. The matrix hydration is fixed at 87.7 wt%. The molar fraction of the cross-linker [MBA] and the silica volume fraction, defined as the volume ratio of silica nanoparticles to the total volume of hybrid hydrogels (calculated using $\rho_{Si} = 2.3 \times 10^6$ g.cm^{-3}), are indicated (see also Table 4 in **SI**).

Nomenclature	[MBA] (mol%)	Φ_{Si} (vol%)
D_SP10_R1	1	10
D_SP10_R05	0.5	10
D_SP10_R01	0.1	10
D_SP10_R0	0	10
D_SP10_R1_pH11	1	10
D_SP10_R01_pH11	0.1	10
D_SP5_R1	1	5
D_SP5_R05	0.5	5
D_SP5_R01	0.1	5
D_SP5_R0	0	5
D_SP2_R1	1	2
D_SP2_R05	0.5	2
D_SP2_R01	0.1	2
D_SP2_R0	0	2
D_SP0_R1	1	0
D_SP0_R05	0.5	0
D_SP0_R01	0.1	0
D_SP0_R0	0	0
A_SP10_R1	1	10
A_SP10_R05	0.5	10
A_SP10_R0	0	10

2.1.3 Sample characterization

For linear polymer chains, sorption isotherms were obtained by dosing the remaining quantity of polymer in the supernatent with a Total Organic Content (TOC) method. Increasing concentrations of polymer were added in a silica suspension of fixed concentration of 0.25 vol% (5 g/L, which is equivalent to an available silica area of 46 m^2). Sufficient time was left for reaching adsorption equilibrium at the silica surface before removing the nanoparticles. The detailed procedure is described in the **SI** file. Solvent NMR relaxometry was also used as a complementary method to quantify adsorption, as described in **SI**.

For hybrid hydrogels, samples were moulded in the glove box. After demoulding, hydro-

gels were immediately characterized or stored in paraffin oil to avoid drying before analysis. The amount of adsorbed polymer was measured by proton NMR relaxometry performed with a low-field, low resolution Bruker Minispec spectrometer. The Modified Magic Sandwich Echo pulse sequence was used to get rid of the so-called dead time of the spectrometer, as described in details in **SI**.[36,37] The modified multiple quanta excitation scheme and analysis procedure proposed by Saalwächter et al. were used to probe the structures of the gel matrices by DQ proton NMR.[38,39]

Swelling ratios at equilibrium were measured in deinonized water with the procedure described in **SI**. The dispersion state of silica nanoparticles was investigated by Small angle X-ray scattering (SAXS) as described in **SI**. Tensile curves were measured in immersion in paraffin oil. Fracture energies were estimated as described in **SI**.

3 Results: tuning polymer adsorption on silica

3.1 Adsorption of linear polymers

The adsorption of PAAm and PDMA linear polymers and copolymers on silica nanoparticles in aqueous solution with a given surface chemistry was first investigated.

The amount Γ of polymer adsorbed on silica nanoparticles (in mg.m^{-2}) is plotted as a function of the polymer concentration C_p (in g/L) in Figure 3(a). In the case of PDMA, as expected, a strong adsorption regime is observed at low coverage with a sharp increase of the adsorbed amount up to $\Gamma \approx 0.5$ mg.m^{-2}. This regime corresponds to the adsorption onto silica surface with nearly all polymer segments interacting with silanol groups (meaning a predominant fraction of polymer chains in train conformations as compared to loops and tails) with amounts in good agreement with those previously reported in the literature[40–42]. This regime is followed by a weaker interaction domain (starting from $\Gamma > 0.5$ mg.m^{-2}) before reaching a plateau value with a $\Gamma_{max} \approx 1$ mg.m^{-2}. Using a heuristic Langmuir isotherm model $\Gamma = \Gamma_{max} K C_p/(1 + K C_p)$, the equilibrium constant is evaluated to be $K \approx 20$ L.g^{-1},

confirming that PDMA strongly interacts with the silica surface.

Increasing the PDMA chain length increases the maximum adsorbed amount Γ_{max} by about 13% (from about 0.95 up to about 1.05 mg.m^{-2}) but it does not qualitatively affect the sorption behavior.

Conversely, PAAm shows nearly zero, or very weak, adsorption, with a plateau value $\Gamma_{max} \approx 0.07$ mg.m^{-2}. As theoretically described by Scheutjens and Fleer[43], the amount of polymers adsorbed at liquid/solid interfaces of course depends on their affinity for the surface, besides the consideration of the strong entropy reduction associated to adsorption. The very small amount of adsorbed PAAm clearly shows a lack of affinity for the silica surface under the given chemical conditions. These differences in adsorption behavior will be further discussed in Section 4.

Adsorption isotherms of copolymers are shown in figure 3(b), together with those of PDMA and PAAm. As expected, adsorption isotherms of the copolymers depend on their acrylamide content and are intermediate between those of pure PDMA and PAAm, reflecting the difference in adsorption ability of each comonomer.

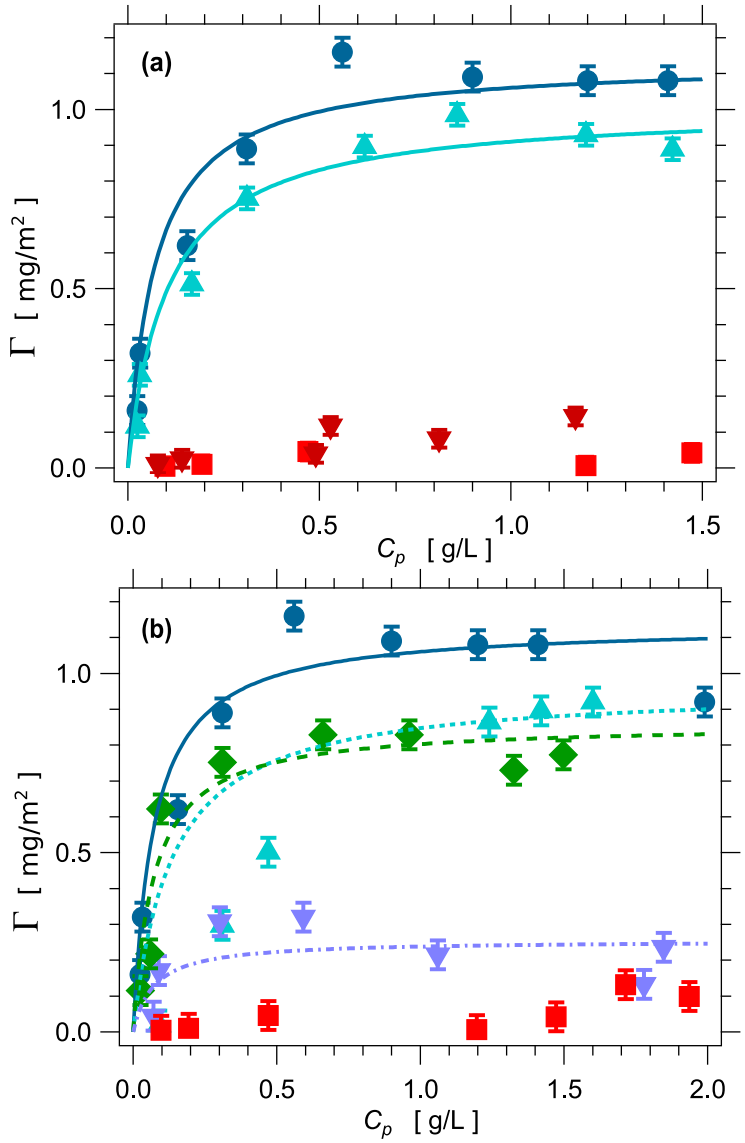

Figure 3: **a.** (a): The adsorbed amount Γ (in mg of polymer per m^2 of silica surface) as a function of the remaining concentration of polymer C_p for PDMA-200 (dark blue dots), PDMA-50 (light blue triangles), PAAm-200 (dark red triangles) and PAAm-50 (red squares). The silica volume fraction is 0.25 vol% and measurements are performed at pH 9. (b): Adsorption isotherms of PAD50/50-50 (blue-green diamonds), PAD20/80-200 (light blue triangles), PAD80/20-200 (light purple starred-shapes), PAAm-200 (red dots) and PDMA-200 (blue dots). The curves are fits with Langmuir isotherms (see text).

The maximum adsorbed amounts Γ_{max} of the homo- and copolymers are reported in Figure 4 as a function of the AAm content in the chains. The Langmuir equilibrium constant K may be expected to decrease as the AAm content increases, reflecting weaker adsorption. However, it is difficult to assess a systematic variation of K as a function of the AAm content

from the curves in Figure 3. All curves were fitted with values of K between about 10 to 20 L.g^{-1}.

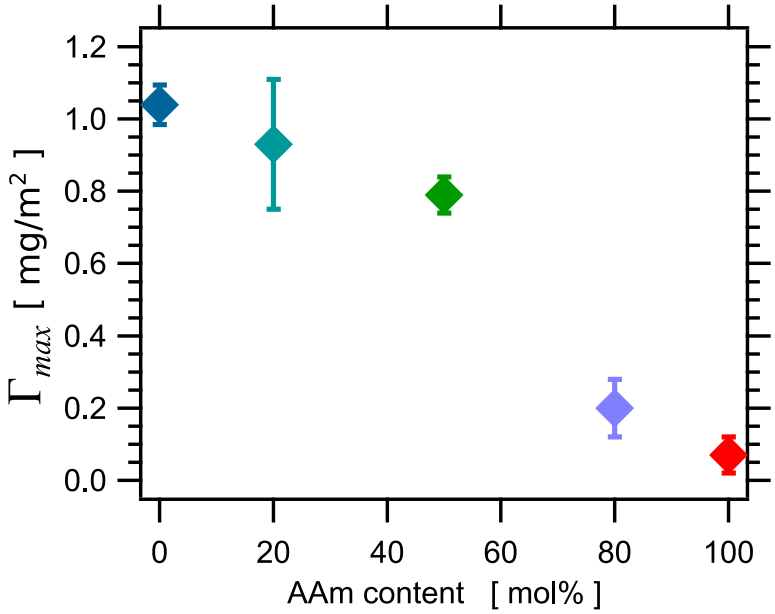

Figure 4: Maximum adsorbed amounts Γ_{max} obtained by fitting the isotherms shown in Figure 3 with Langmuir-type isotherms for PAAm-200 (red), PDMA-200 (dark blue), PAD20/80-200 (light blue), PAD50/50-50 (green) and PAD80/20-200 (light purple), in mg/m^{-2} for 0.25 vol% silica at pH 9. Note that PAD50/50-50 has $M_n \approx 150000$ g/mol, which is comparable to other samples (see Table 1).

Another method is based on the impact of adsorption on the solvent (water) mobility, which in turn affects the solvent NMR relaxation time, as described in **SI**.[44–46] The NMR proton relaxation rates R_2 of water were measured in solutions containing different PDMA concentrations between 0.05 and 0.5 wt% and silica contents from 0 to 10 vol%. The relative relaxation rates $R_{sp} = R_2/R_2^0$, where R_2^0 is the relaxation rate of pure water, are plotted as a function of the silica volume fraction in Figure 5.

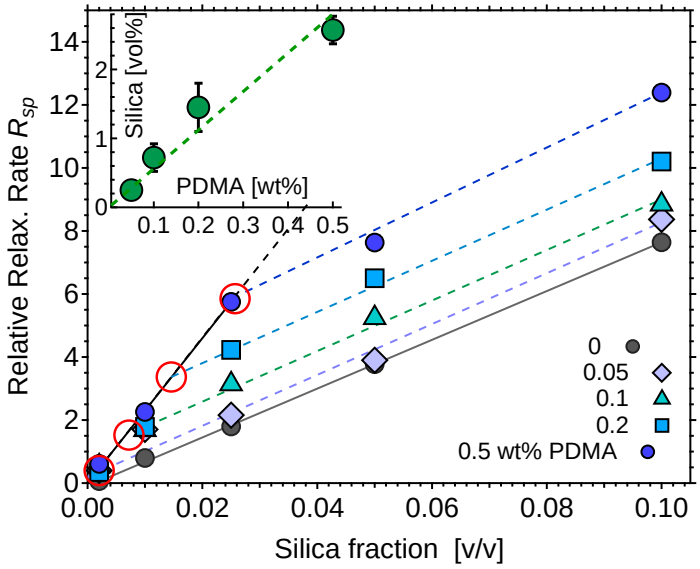

Figure 5: The relative relaxation rates R_{sp} as a fonction of the silica volume fraction for PDMA solutions at several PDMA concentrations as indicated in the legend. Red circles emphasize the intercept between the two linear regimes in each curve. The inset shows the relationship between the silica and PDMA concentrations at the transition point.

For each polymer concentration, two linear domains are clearly identified in the curves of Figure 5. In the first regime (low silica concentration), the slope is much larger than for the bare silica. This slope seems to be independent of the PDMA concentration. Then, breaks in the slopes occur at silica concentrations which increase as the PDMA concentration increases. Since the polymer in solution alone has negligible effect on the water relaxation time, this behavior may be attributed to polymer adsorption. Given the relative amounts of polymer and silica in the various solutions, it appears that the first regime corresponds to the adsorption plateau in Figure 3, with silica particles fully covered by PDMA. In the second regime, the slope is comparable to that of bare silica. When silica is in excess, all the available polymer is adsorbed and the overall solvent dynamics is driven by interactions with bare silica. The roughly linear relationship between the silica and PDMA concentrations at the transition point is shown in the inset in Figure 5. From the slope of this relation, the adsorbed PDMA amount is found to be $\Gamma_{PDMA} \approx 0.9$ mg/m^2, assuming that the silica density is 2.3 g/cm^2 and the specific surface 100 m^2/g. This value is perfectly consistent

with the results of TOC measurements (see Figure 4). One may wonder whether the slight difference in adsorption values measured by both methods is significant. It may be related to the fact that loops and tails do not contribute significantly to the reduction inmobility, hence to the reduction of NMR relaxation rate of the solvent, while they contribute to TOC measurements. Based on the measured figures, it might be concluded that about 85% of the adsorbed polymer segments would have a strongly reduced mobility. Finally, the same experiments carried out on PAAm-silica solutions do not show the same behavior. Curves of the relaxation rate as a function of the silica content do not show the two distinct regimes characteristic of adsorption.

3.2 Polymer adsorption in hybrid hydrogels

NMR relaxometry is a quite direct way to characterize adsorption in hybrid hydrogels, as adsorbed monomers and those embedded in the gel network in solution should exhibit a dramatic difference in mobility, which in turn corresponds to a dramatic difference in transverse NMR relaxation time scales. A slow decay of the NMR relaxation function corresponds to the response of a mobile polymer. Conversely a rapid decay shows the presence of less mobile polymer. However, for a rigid polymer exhibiting slow dynamics, the corresponding fast decay cannot be measured quantitatively by simple single-pulse transverse relaxation (so-called FID) measurements, due to the dead time of the spectrometer. Hence, the Magic Sandwich Echo (MSE)-refocused transverse relaxation was used to recover the whole NMR relaxation function at short times (see **SI**).[36,37] Besides, gels were prepared in D_2O to measure selectively the response of the protons for polymer chains.

In PDMA-based hybrid gels, a fraction of the NMR proton signal relaxes very fast as compared to the signal of a mobile polymer, within a time scale of order 0.05 ms, as shown in figure 6. The unfilled gels do not show this fast relaxing contribution (see **SI**). This directly indicates that a fraction of rigid (immobilized) polymer is indeed present in PDMA-based hybrid hydrogels. This immobilized polymer fraction is interpreted as due to polymer

adsorption onto nanoparticles. Observing two well-separated contributions in the signals indicates that there is no exchange between the corresponding populations of chain segments on the observation time scale, that is of the 0.1 to 1 ms time scale. This indicates that adsorption must be considered to be permanent on that time scale.

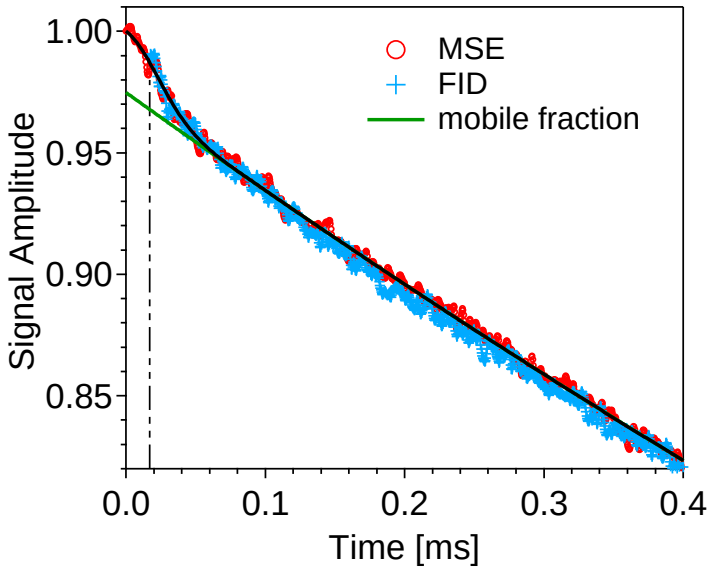

Figure 6: FID (blue crosses) and MSE-refocused FID (red symbols) of sample D_SP10_R01. The black curve is the fit with Eq. 1, the green curve corresponds to the long time contribution only, which corresponds to the mobile fraction. The dashed vertical line indicates the dead-time of the spectrometer ($\approx 17\mu$s), within which the FID signal is not detected.

Precisely quantifying the relative amount and the mobility of the corresponding polymer fraction requires careful analyzis of the signal, as the relative amplitude of the rigid (fast relaxing) contribution is not fully quantitative in the MSE sequence, while the amplitude of the mobile part is not significantly affected by the MSE sequence. To be quantitative, the amplitude of the signal from the rigid fraction in the material obtained in a MSE sequence with a refocusing delay $\tau_{MSE} = 4$ μs should be multiplied by a factor about 1.2. This factor was estimated by extrapolating the MSE signal amplitude obtained on dry PDMA at 308 K (which is below the glass transition temperature of the polymer) to a refocusing delay $\tau_{MSE} = 0$ μs, according to a procedure detailed in **SI**.

The corrected MSE relaxations functions (normalized to one at $t = 0$) were fitted in the

time interval 0 - 0.25 ms with a two-component function of the form

$$\frac{MSE(t)}{MSE(0)} = \varphi_r \exp\left[-\frac{M_2 t^2}{2}\right] + (1-\varphi_r)\exp\left[-\left(\frac{t}{T_{2eff}}\right)^b\right] \quad (1)$$

where φ_r is the rigid (adsorbed) fraction. Beyond typically 0.25 ms, the measured function is dominated by field inhomogeneities and is not fully representative of the actual intrinsic relaxation function of the polymer. The fast decaying part of the signal at short times, associated with the rigid adsorbed fraction φ_r, is fitted with a Gaussian-type function. It has the same shape, with the same value of the second moment $M_2 \approx 1465$ kH^2, as for the dry polymer, with no significant, systematic dependence on the cross-linker amount. The signal from the mobile part of the polymer decays on a much longer time scale. It can be fitted with a heuristic stretched exponential function $\exp\left[-(t/T_{2a})^b\right]$, with b very close to one. However, residual H_2O contained in the monomer also contributes to the overall ^{1}H NMR signal and must be taken into account to get a quantitative estimate of the amount of adsorbed polymer.

Adsorbed amounts may be predicted based on the values of Γ_{max} determined with linear polymer chains (Section 3.1). Predicted amounts (calculated with a specific surface of silica nanoparticles $S_{spe} = 100$ m^2/g and $\Gamma_{max} = 1$ mg/m^2) are reported in Table 4 for the samples with 10 vol% silica and increasing fractions of MBA cross-linkers.

Table 4: The measured rigid (adsorbed) polymer fraction φ_r in PDMA hybrid gels with 10 vol% silica measured by NMR (see Figure 6 and equation 1) and the predicted fraction φ_{th} based on the results of Section 3.1. φ_{th} was calculated using Γ_{max}= 1 mg/m^2 and a silica specific surface of 100 m^2/g.

Sample	φ_{th} (wt%)	φ_r (wt%)
D_SP10_R0	2.87	3.72 ± 0.4
D_SP10_R01	2.87	2.25 ± 0.3
D_SP10_R05	2.87	2.4 ± 0.5
D_SP10_R1	2.87	2.4 ± 0.7

Adsorbed amounts obtained from NMR measurements φ_r are roughly consistent with the ones φ_{th} calculated from adsorption isotherms of linear chains, which do not take the cross-

linking of the network into account. Overall, the adsorbed amounts tend to decrease as the chemical cross-linker content increases. This may indicate that adsorption and cross-linking occur concomitantly and are in competition. Indeed, a higher cross-linking density of the network should effectively yield additional constraint on network chains, thus decreasing the adsorbed fraction of polymer.

3.2.1 Inhibiting polymer-filler interactions

It was shown in Section 3.1 that linear PAAm chains do not adsorb on silica nanoparticles. This behavior is confirmed in hybrid hydrogels. No short time signal corresponding to a rigid fraction is observed in PAAm-based hybrid gels. The same is true in PDMA-based hybrid gels synthesized at pH 11, in which PDMA adsorption is inhibited. These results are illustrated in figure 7. Thus NMR relaxometry measurements in hybrid gels directly confirm both the non-adsorbing behavior of PAAm and the change of affinity towards silica surface of PDMA synthesized at pH 11.

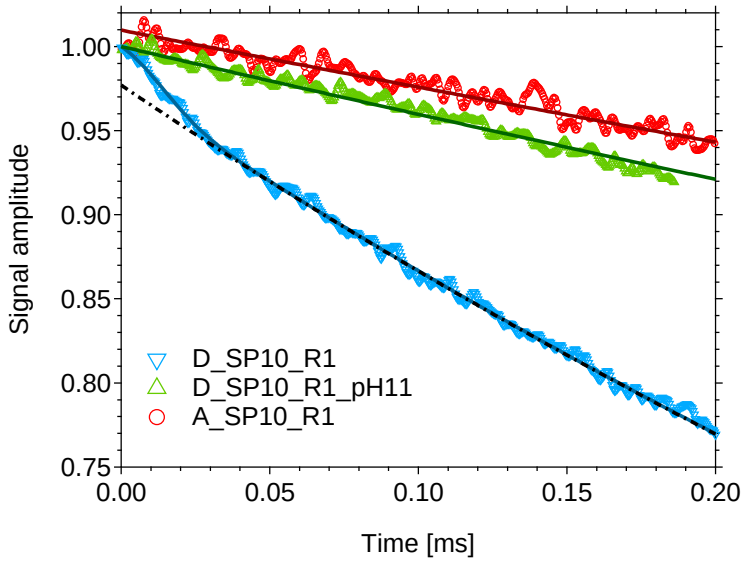

Figure 7: MSE-refocussed FID of samples D_SP10_R1 (blue), D_SP10_R1_pH11 (green) and A_R1_SP10 (red). Plain curves are fits with Eq. 1. The dashed curve is the long time contribution (mobile fraction) in sample the mobile D_SP10_R1. Samples D_SP10_R1_pH11 and A_R1_SP10 do not contain a rigid (adsorbed) fraction.

3.2.2 Impact of chemical cross-linker content

Polymer adsorption on silica particles and cross-linking may enter in competition during the processing of hybrid gels. The MSE relaxation functions measured in a series of hybrid hydrogels with 10 vol% silica and various cross-linker amounts are shown in figure 8. In all cases the signal could be well fitted with two distinct components as in Eq (1), with a Gaussian contribution at short times and an apparent exponential fitting (within the observation time range considered here) for the contribution at longer times corresponding to the mobile polymer fraction. For this contribution, the relaxation rate strongly increases as the cross-linker content increases. This is due to the fact that the relaxation function of a network contains a contribution from the residual dipolar coupling, related to the cross-link density. More crosslinks introduce more topological constraints in the chains, which results in larger residual dipolar interactions and a larger relaxation rate (see Section 3.3 below).

All samples exhibit an immobilized polymer fraction. The corresponding signals are similar, with $M_S \approx 1300$ kH^2. The adsorbed polymer fraction does not seem to depend significantly on the chemical cross-linker content. In all cases, the observed adsorbed amounts are consistent with the ones calculated without taking into account the cross-linking density of the polymer network.

For silica contents below 10 vol%, the immobilized polymer fraction was distinctively smaller and could not be precisely quantified. This might be consistent with the mechanical properties reported for those systems, with significant reinforcement observed for silica volume fractions of 10 vol% or higher.[7]

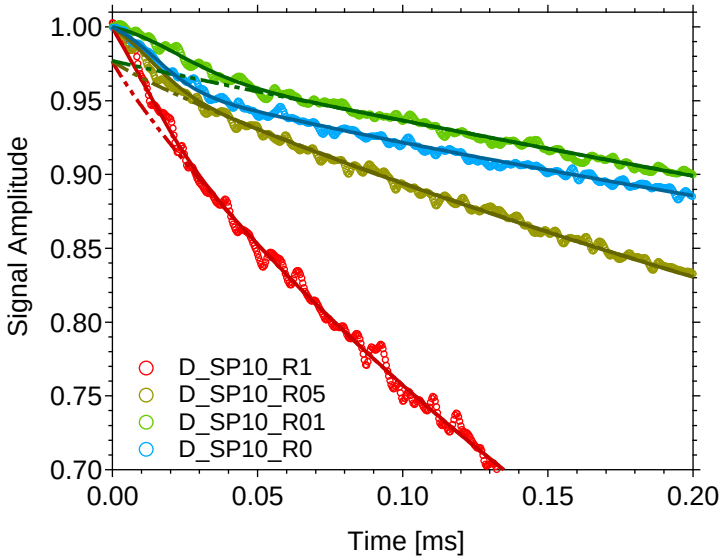

Figure 8: MSE-refocussed FID curves of the D_SP10_R_z set of samples with z= 0 (blue), 0.1 (green), 0.5 (greenish yellow) and 1 (red) mol% Plain curves are fits with Equation 1. Dashed curves are the long time contributions (mobile fraction) for the chemically cross-linked samples.

3.3 Effect of adsorption on the apparent crosslink densities of hybrid hydrogels

In this section we compare the apparent crosslink densities as measured by DQ proton NMR, in the unfilled and hybrid gels. Let us recall that samples were prepared here in deuterated water to selectively observe the polymer signal.

Representative examples of the raw DQ and reference signals and the detailed analysis procedure of DQ results are presented in **SI**.

The first step in the analysis is to subtract the signal from the non-elastically active part of the samples (the so-called network defects). In PDMA hybrid gels, the fraction of defects was evaluated between 5 and 8%. This is qualitatively consistent with the value of the extractible content not exceeding 2 % measured in swelling experiments. In the physical (uncrosslinked) PDMA hybrid gel, the fraction of defects is about 16 %, which qualitatively agrees with a gel only weakly and reversibly cross-linked by silica nanoparticles.

Conversely, in PAAm hybrid gels, nearly 50% of the signal seems to possess a long relaxation time, which makes the evaluation of network defects hard to perform. In fact, TGA analyses conducted on the AAm monomer have revealed the presence of about 40 wt% bounded water. Besides, the primary amide moiety of PAAm can exchange its protons with the deuterium atoms of the surrounding solvent. Assuming complete exchange of these protons with the excess water in the gels, the only protons contributing to the DQ signal are the three ones linked to the skeleton, that cannot exchange. This explains the difference between the PDMA and PAAm signals.

Normalized DQ curves of PDMA and PAAm hybrid gels for the SP10 set of samples (10 vol% silica) are shown in figure 9.

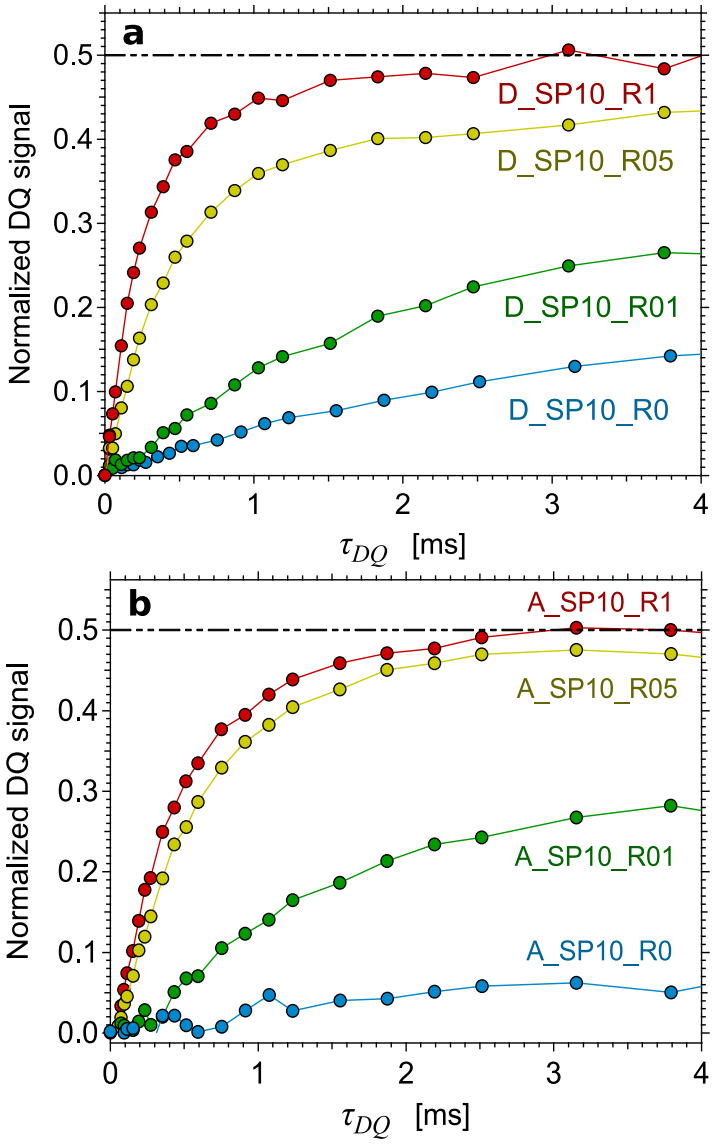

Figure 9: **a.** Normalized DQ signals as a function of the DQ evolution time: **a**: PDMA-based hybrid gels D_SP10_R_z with $z = 0$ (blue), 0.1 (green), 0.5 (yellow) and 1 mol% (red); **b.** PAAm-based hybrid gels A_SP10_R_z, with $z = 0$ (blue), 0.1 (green), 0.5 (yellow) and 1 mol% (red).

The normalized DQ curves of PAAm unfilled and hybrid gels (at $R = 1$ mol% and silica content 0 and 10 vol%) are shown in Figure 10. The comparison with the PDMA hybrid gel (D_R1_SP10) with the same MBA molar ratio and silica content shows that D_{res} remains lower (0.75 for PAAm and 1.38 for PDMA), indicating that silica does not yield additional cross-linking points to the structure of PAAm gels. The results confirm the hypothesis of inert fillers embedded in the polymer matrix as evidenced by MSE measurements conducted

on those samples.

The D_{res} of the unfilled PAAm gel (A_R1_SP0, $D_{res} = 0.80 \pm 0.04$) seems to be a little higher than that of (A_R1_SP10, $D_{res} = 0.75 \pm 0.04$). This suggests that silica, besides acting as an inert filler, may partly inhibit cross-linking which could be a further reason for the observed decrease of the mechanical properties of these compounds[13]. This may result in the presence of a depletion zone formed around the silica nanoparticles. Observing this depletion zone, however, would require additional experiments providing some spatial resolution.

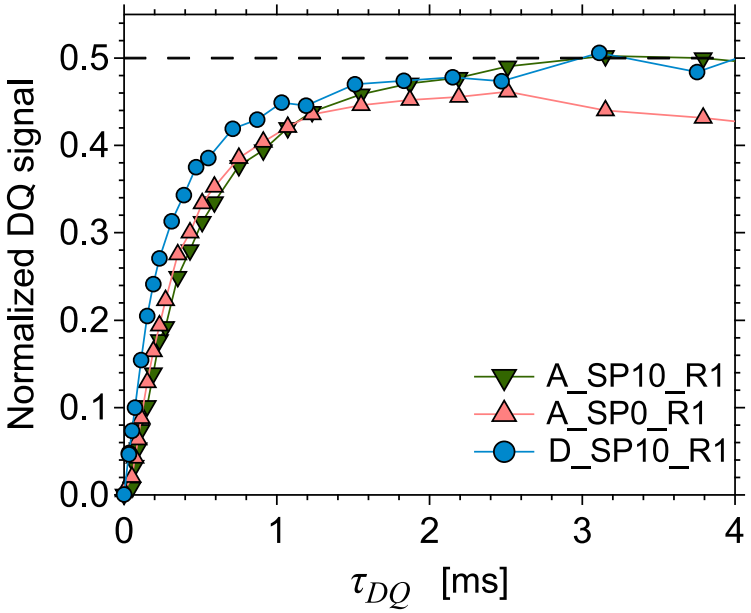

Figure 10: Normalized DQ signals of A_SP10_R1 and A_SP0_R1. D_SP10_R1 is displayed as a comparison.

The obtained D_{res} values, extracted from the initial slope of the normalized DQ signals, are plotted in figure 11 as a function of the cross-linker content.

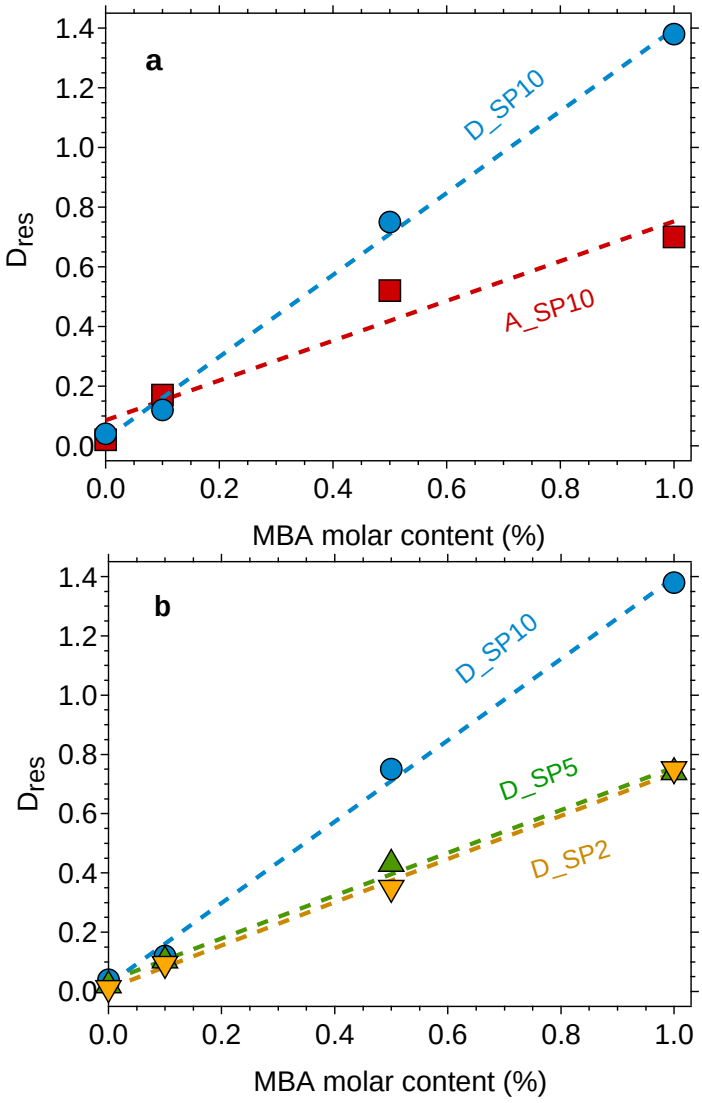

Figure 11: **a**: D_{res} values for PDMA (blue dots) and PAAm hybrid gels (red squares) as a function of the cross-linker (MBA) molar ratio at a fixed silica content of 10 vol%. **b**: D_{res} values for PDMA hybrid gels as a function of the MBA molar ratio for silica contents 10 vol% (blue dots), 5 vol% (green triangles) and 2 vol% (yellow down triangles) as a function of the chemical cross-linker content. Dashed lines are linear fits. D_{res} values are obtained as the slope of the corresponding normalized DQ signals at short times.

First, PDMA and PAAm hybrid gels with a constant silica volume fraction 10 vol% are compared in figure 11(a). D_{res} increases as the cross-link density (MBA content) increases in both PDMA and PAAm gels. For the PDMA hybrid gel series, D_{res} is roughly proportional to the MBA content, with perhaps a non-zero, even though small, value at zero MBA content.

This behavior is quite similar to what is generally observed in crosslinked elastomers, in which the non-zero intercept is commonly interpreted as the contribution from entanglements.[47,48] For the PAAm series, the same trend is observed, with a larger scattering of data points however.

Secondly, when comparing PDMA and PAAm hybrid gels at the same MBA content, the PDMA gel has a larger D_{res} value as compared to the PAAm gel. This may be attributed to the interactions between PDMA and silica acting as supplementary effective cross-linking points, these supplementary cross-linking points being absent in the case of PAAm-based hybrid gels.

However, this increase is relatively moderate and, quite surprisingly, it does not correspond to an additive additional contribution proportional to the overall silica surface introduced in the hybrid gels (which would correspond to parallel lines in Figure 11(a)).

As shown in figure 11(b), in PDMA hybrid gels for a given MBA content, D_{res} increases as the silica amount increases. This confirms that silica nanoparticles do contribute to the effective cross-linking of the network. This indicates that polymer/silica adsorption sites play the role of transient effective cross-link sites and contribute to the elasticity of the systems.

As shown in figure 11(b), in PDMA hybrid gels for a given MBA content, D_{res} increases as the silica amount increases. However, as noted before, this increase does not correspond to an additional number of crosslinks proportional to the overall silica surface area introduced in the hybrid gels (which would correspond to parallel lines in Figure 11(b)). For each MBA content, it rather seems to correspond to a multiplicative contribution, with a factor of order 2 to 4 (depending on the MBA content) as compared to the unfilled gel. This confirms that silica nanoparticles do contribute to the effective cross-linking of the network, but in a more complex way than simply adding polymer/silica adsorption sites as effective additional crosslinks. The effect on the network topology and elasticity is more complex. In the context of elastomers, in the limit of low crosslink densities and at high temperature, it has been suggested that the entanglement density detected in NMR may increase as the

crosslink density increases.[49] As the studied gels, when compared to elastomers, should effectively correspond to low crosslink density/high temperature, such an effect may perhaps contribute to the complex interplay between silica surfaces and network architecture.

Finally, the normalized DQ curves of PDMA synthesized at pH11 are shown in figure 12 and indicate a behavior similar to that of PAAm with decreased D_{res} values at equivalent chemical cross-linker contents, as show in table 6. On the other hand, the synthesis at higher pH does not lead to a higher fraction of network defects (i.e, pending chains, unreacted moieties), indicating that the difference of behavior is only due to the change in the silica surface chemistry. Tuning the surface chemistry of silica nanoparticles clearly impacts the effective cross-linking density of the PDMA network, underlying its crucial importance for mechanical reinforcement.

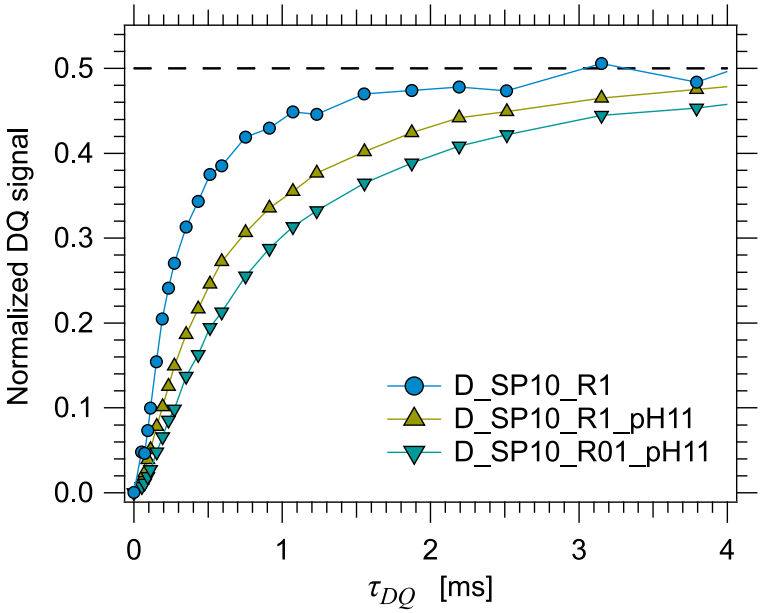

Figure 12: DQ curves of D_SP10_R1_pH11 (green triangles) and D_SP10_R01_pH11 (green dots). D_SP10_R1 is displayed as a reference (blue dashed line).

3.3.1 Impact of silica on PDMA matrix

The impact of silica on PDMA hybrid gels on the normalized DQ signals remains weaker than that of chemical cross-linker as displayed in figure 13 with a significant impact noticed for a silica content of 10 vol%. The obtained D_{res} values are relatively similar for PDMA

gels with silica content ranging from 0 to 5 vol% as indicated in Table 5.

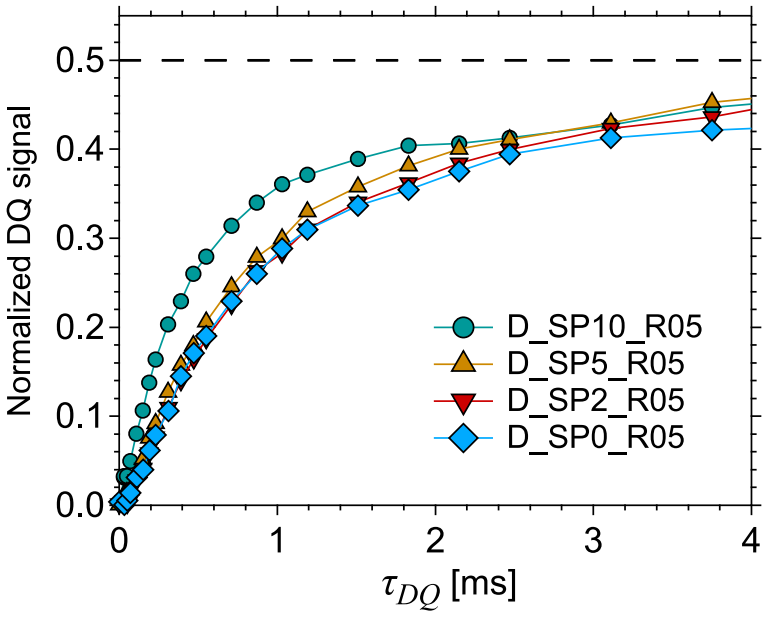

Figure 13: DQ curves of hybrid PDMA at fixed cross-linker ratio 0.5 mol% D_SP10_R05 (blue-green) and D_SP5_R05 (yellow), D_SP2_R05 (red) and D_SP10_R05 (light blue). D_{res} is almost the same for silica content below 10 vol% indicating weak impact of silica on the global network cross-linking density for low silica amount.

These results are qualitatively consistent with previous results on the mechanical behavior of PDMA hybrid gels with various silica contents, where a significant reinforcement was reached at a silica volume fraction of about 10 vol%, both in terms of the modulus, with a marked deviation from the Guth and Gold model[50], and in terms of the strain and stress at break[8]. Still, one may wonder whether the sensitivity of the experiment is high enough to quantify the impact of silica nanoparticles on the apparent cross-link density at silica contents 5 vol% and below. A possible mechanism to explain that D_{res}, as well as mechanical reinforcement, do not vary linearly as a function of the silica content might be the formation of bridges by chains adsorbed on two neighboring particles, which may form beyond some critical volume fraction corresponding to a critical average particle-particle distance. However, assessing this hypothesis would certainly require further investigation, using e.g. rheology.

Table 5: Extracted D_{res} values from the curves displayed in figure 13 for PDMA hybrid gels at constant MBA molar ratio of 0.5 mol% and various silica content (0, 2, 5 and 10 vol%).

Sample	Extracted D_{res}
D_SP10_R05	0.73
D_SP5_R05	0.43
D_SP2_R05	0.41
D_SP0_R05	0.43

Table 6: Extracted D_{res} values from the curves displayed in figure 12, for PDMA hybrid gels synthesized at pH 11 at MBA molar ratio of 1 and 0.1 mol% and constant silica content (10 vol%).

Sample	Evaluated defects (%)	Extracted D_{res}
D_SP10_R1_pH11	4.5	0.73
D_SP10_R01_pH11	6	0.43

3.4 Effect of polymer adsorption on the mechanical behavior

In order to discriminate the effect of polymer/silica interactions, it must be checked that changing the nature of the polymer does not affect the dispersion state of silica nanoparticles, which would considerably impact the mechanical response of the hybrid gels as well. SAXS experiments were carried out to probe the dispersion state of the silica nanoparticles within the polymer matrix.

3.4.1 Dispersion state of silica nanoparticles

Figure 14 shows SAXS signals of the NC_D, NC_A and NC_A_{90}-D_{10} samples (ϕ_{Si} = 20 vol%). All curves superimpose perfectly in the high-q regime (typically $q \geq 0.025$ Å^{-1}) and show an overall q^{-4} dependence in this regime, which indicates that particles have the same size and morphology (spheres of mean radius R = 13.4 nm with a narrow gaussian distribution $\sigma_{Gauss} = 0.13$) in the three samples. The general shape of the curves is very similar to the one of the silica suspension at ϕ_{Si}=0.20 while the bump associated to hard sphere repulsion is not as pronounced as in the Ludox suspension (see **SI**). At low q values ($q \leq 0.01$ Å^{-1}), the intensity is slightly higher for PAAm-based hybrid gels (NC_A and NC_A_{90}-D_{10}), pointing

to slightly lower repulsion between silica particles, indicating that silica is more prone to aggregate in these PAAm-based hydrogels than in the PDMA gel. Curves were fitted with a sticky hard sphere model(see **SI**). Values found for the stickiness show the larger decrease of repulsions between silica particles in the presence of adsorbed PAAm than with PDMA.

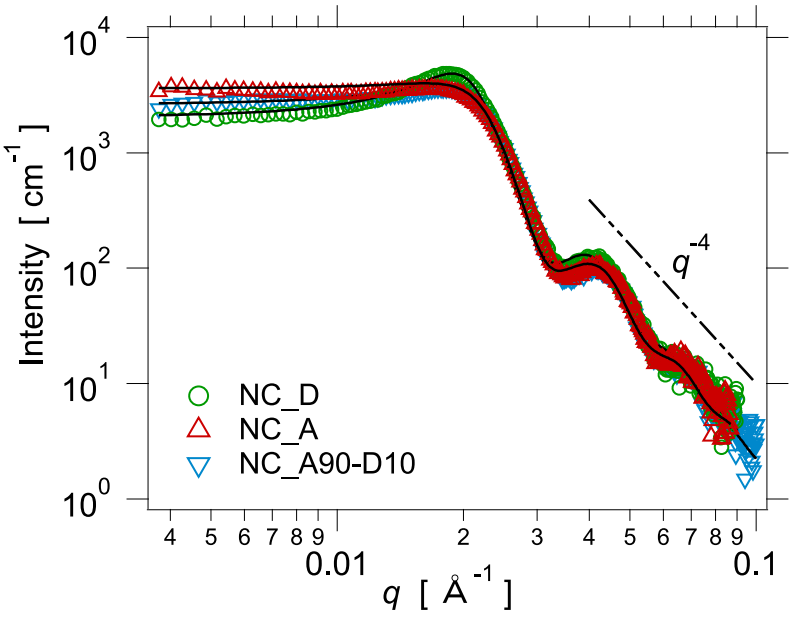

Figure 14: SAXS intensities measured in NC_D (green circles), NC_A (red triangles) and NC_A_{90}-D_{10} (turquoise down triangles) samples at 20 vol% silica. Black solid curves are fits based on the sticky hard sphere mode (see **SI**).

3.4.2 Mechanical response

Typical stress-strain curves are shown in figure 15 for a strain rate $\dot{\epsilon} = 0.06$ s^{-1}. Both NC_A and NC_D exhibit homogeneous deformation without necking. NC_D displays a highly non-linear behavior with a marked "S-shaped" curve indicating strong deviation from the classical model of rubber elasticity, with a softening at intermediate strain (around $\epsilon = 0.5$) and a strain hardening at higher strain indicating finite extensibility of the polymer chains. As previously reported, the stretchability is highly improved ($\epsilon \approx 700\%$) compared to the one of chemical PDMA gel.

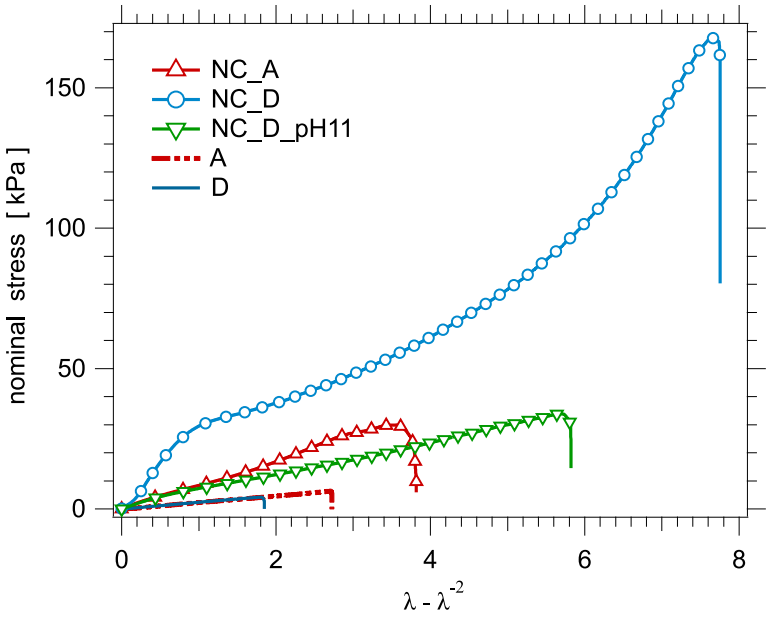

Figure 15: Stress-strain curves of PAAm and PDMA hybrid gels and of the PDMA hybrid gel synthetized at pH = 11, with 20 vol% silica. The curves from the PDMA and PAAm unfilled gels are shown for comparison. All samples are cross-linked with 0.1 mol% MBA. Tensile tests were conducted at 0.06 s^{-1}.

The linear tensile modulus can be obtained from tensile experiments at low strain and the values are reported in Table 7 for NC_D and NC_A and the corresponding unfilled gels.

The impact of filler in a rubbery matrix was adressed by Guth and Gold and Simha[50,51], from purely elastic considerations (i.e, an incompressible polymer matrix and fillers treated as cohesive hard spherical particles). They predicted an evolution of the linear tensile modulus at low strain for low volume fractions of filler (ϕ_{Si}¡ 0.2) according to the following equation:

$$E = E_0(1 + 2.5\phi_{filler} + 14.1\phi_{filler}^2) \quad (2)$$

with E, the initial modulus, E_0, the unfilled matrix modulus and ϕ_{filler}, the particle volume fraction. It was already shown that this model clearly underestimates the value of E in the case of strong interactions between the matrix and the fillers, that serve as multiple anchor points for the polymer chains providing an increase of the elastically active chains per unit of volume.[52] Note that, according to Figure 11, the effective cross-link density is increased

by a factor of about two in the presence of silica in PDMA hybrid gels. Beyond the Guth and Gold and Simha factor, this should further increase the modulus E_0 by a factor of about 2, as indicated by the open black diamond in Figure 16. In any case, for the NC_D gel and for gels with low AAm contents, the stiffness is significantly higher than the Guth and Gold prediction. The acrylamide content in hybrid hydrogel leads to a significant decrease of the gel stiffness from about 100 kPa to 23 kPa for a constant silica volume fraction of 0.203 as depicted in Figure 16. The experimental modulus value of NC_A is in good accordance with the Guth and Gold prediction ($\approx$ 22.5 kPa for a silica volume fraction of 0.203), confirming once more the lack of interactions between PAAm and silica nanoparticles and their strong impact on the gel stiffness as shown in table 7.

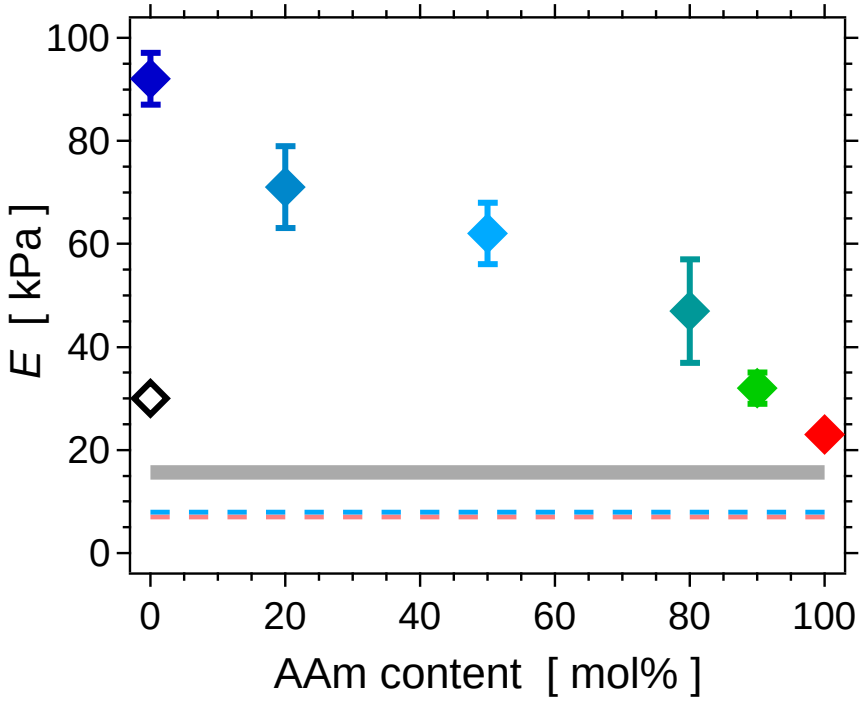

Figure 16: Initial modulus of hybrid gels containing various contents of DMA and AAm at 0.203 v/v silica, conducted at $0.06s^{-1}$. Dashed lines represent the linear tensile modulus of the chemical gels, MA_R01 (pink) and MD_R01 (blue).The plain grey line represents the Guth and Gold theoretical prediction for a silica volume fraction $\phi_{Si} = 0.203$. The open black diamond is the Guth and Gold prediction, taking the additional cross-link density of the matrix due to silica particles in the PDMA hybrid gel into account.

Table 7: Experimental values of initial modulus E, compared to the predicted value calculated from the Guth and Gold model for a silica volume fraction of 0.203. Silica volume fraction was defined as the volume ratio of silica nanoparticles to the total volume of hybrid hydrogels, fixed at 0.203 for all compositions (using $\rho_{Si} = 2.3 \times 10^6 g.cm^{-3}$).

Sample	w_{AAm}(mol. fraction)	E (kPa) at $\dot{\epsilon}$= 0.06 s^{-1}	E_{calc} (Guth and Gold)
NC_D	0	92±5	22.5
NC_A	1	23±1	22.5
NC_A_{90}-D_{10}	0.9	32±3	22.5
NC_A_{80}-D_{20}	0.8	47±10	22.5
NC_A_{50}-D_{50}	0.5	53±6	22.5
NC_A_{20}-D_{80}	0.2	71±8	22.5

The ability of the hybrid networks to relax stress concentration by dynamic exchanges between adsorbed and unadsorbed polymer segments is permanently disabled when the interacting monomer is substituted with one displaying lower affinity.

3.4.3 Fracture energy

Fracture energies (or equivalently energy release rates) calculated from single-edge notched tensile tests (see **SI**) for NC_A and NC_D at various strain rates are shown in figure 17. Note that the crack propagation rate is not controlled in these experiments, so that an apparent G_1c at onset of unstable propagation is calculated.

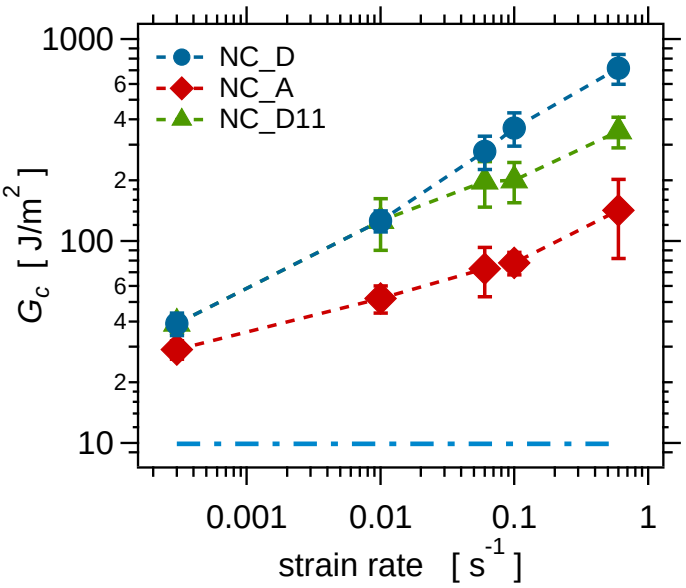

Figure 17: Calculated fracture energies for NC_A (red diamonds), NC_D (blue dots) and NC_D synthetized at pH 11 (green triangles) for various strain rates ($\dot{\epsilon} = 3 \times 10^{-4}$, 0.01, 0.06, 0.1 and 0.6 s^{-1}). The fracture energy of a chemical gel (MD_R01, $G_{1c} = 9.92$ J/m^2) is also shown as a reference (blue dashed line).

Adding silica nanoparticles in the presence of an interacting PDMA polymer matrix (NC_D) significantly increases the energy release rate, in all the investigated strain rate range. As the polymeric matrix has a low cross-link density, the effect of the silica nanoparticles is quite large. Comparatively, PAAm hybrid gels with the same cross-linker molar content have much smaller fracture energies. A comparison can be done with the Lake and Thomas's estimation[53] for the threshold energy G_{LT} necessary to propagate a crack in unfilled elastomers :

$$G_{LT} = \Sigma J N_c$$

with Σ the surface density of chains crossing the fracture plane, N_c is the number of monomer units between cross-links and J is the required energy to break one covalent bond. This model is based on the assumption that the transmitted load brings each polymer strand crossing the interface close to its maximum free energy, which gives a calculated value of 1.2 J/m^2 for 500 monomer units between two cross-link points (0.1 mol %). This model gives a rough

estimate of the fracture energy for chemically cross-linked samples. However, it is clearly not appropriate to describe fracture in hybrid gels, which involves large deformations, crack blunting and presumably large a dissipative volume contributing to the overall measured fracture energy.

Table 8: Experimental values of fractures energies at various strain rate for NC_D, NC_A and MD_R01 (chemical gel displayed as a reference) compared to the Lake and Thomas calculation estimated at 1.2 J/m^2.

strain rate (s^{-1})	G_{1c} NC_D (J/m ^{2})	G_{1c} NC_A (J/m^2)	G_{1c} MD_R01 (J/m^2)
3.10^{-4}	39 ±5	29 ±3	-
0.01	126 ±15	52 ±8	-
0.06	278 ± 52	73 ± 20	10 ± 2
0.1	363 ± 68	78 ± 10	-
0.6	717 ± 77	142 ± 60	-

Unfilled elastomers show an increase of fracture energy as the strain rate increases[54], which is related to the viscoelasticity of the materials. As the strain rate increases, a larger fraction of the energy is dissipated, which means that a higher overall mechanical energy must be provided to break the sample. However, this increase is dratically more pronounced in PDMA (NC_D) hybrid hydrogels. Conversely, PAAm hybrid gels based on non-interacting monomer display comparatively lower fracture energies and, moreover, a much less pronounced variation as the strain rate increases.

For PDMA hybrid gels synthetized at pH = 11, in which adsorption is inhibited, the values of fracture energies and the dependence on the strain rate are intermediate between those in PAAm and PDMA hybrid gels synthetized at pH = 9. A small fraction of PDMA-silica interactions may still be effective at high pH values.

These experiments emphasize the key role played by polymer adsorption, which involves dynamic exchanges between adsorbed and unadsorbed polymer segments, in dissipative processes and thus in gel toughening.

4 Discussion

Model hybrid gel systems were carefully designed to selectively tune the polymer-particle interactions while maintaining similar dispersion states of the nanoparticles. Indeed, changing polymer-particle interactions dramatically affects the dispersion state of nanoparticles, as promoting adsorption of a polymer layer may contribute to create a *repulsive* interaction potential between nanoparticles, while, conversely, inhibiting adsorption may induce polymer depletion, thus contributing to create an *attractive* interaction potential between nanoparticles. In this work, this problem was circumvented by polymerizing and cross-linking the gels in-situ. The polymer adsorption on silica nanoparticles for varying polymer-particle affinity was first separately investigated in solutions of linear polymers. The effect of adsorption on the mechanical and fracture properties was then thoroughly investigated in hybrid gels of various compositions in terms of both cross-link density and silica volume fraction.

The study of the adsorption of linear polymer chains shows that PAAm have much less affinity than PDMA towards the silica surface under specific conditions (pH, size of nanoparticles, weak ionic force). As adsorption between silica and poly(N-alkylacrylamides) proceeds through a balance of hydrogen-bonding, a possible explanation could be that, as PAAm is better solvated by water than poly(N -alkyacrylamides), solvent-polymer interactions prevail on polymer-nanoparticle interactions, leading to the experimentally observed decreased adsorption of PAAm. This was suggested by Perrin et *al.*, who used molecular dynamics simulations to model the possible role of the solvent, and also by the theoretical work conducted by Molinari et *al.*[21,55] This last argument is supported by the results obtained for PDMA hybrid gels synthesized at pH 11, in which the mechanical properties are decreased compared to those of PDMA hybrid gels synthetized at pH 9, probably induced by the change of silica surface chemistry. An somehow similar approach has been recently proposed to rationalize the adsorption of polymers on the surface of silica nanoparticles in solution in a solvent as a function of the respective interactions between the three components of the system.[56] Adsorption of a polymer in solution in a solvent can be predicted based on the consideration of

an adsorption parameter χ_S defined by $k_BT\chi_S = \sqrt{v_m^{(S)} v_m^{(P)}} \left(\vec{\delta_P} - \vec{\delta_S}\right) \left(\vec{\delta_N} - \vec{\delta_S}\right)$ computed from the relative locations of the solvent (subscript S), polymer (subscript P), and nanoparticles (subscript N) in the 3D Hansen space, represented by the solubility vectors $\vec{\delta_S}$,$\vec{\delta_P}$ and $\vec{\delta_N}$ respectively. $v_m^{(S)}$ and $v_m^{(P)}$ are the molecular volumes of the solvent and the monomer respectively. Basically, this parameter is related to the respective distances of the solvent and polymer representative points to that of the particle in the Hansen space. The factor $\left(\vec{\delta_P} - \vec{\delta_S}\right)$ describes the monomer-solvent affinity. The second factor $\left(\vec{\delta_N} - \vec{\delta_S}\right)$ corresponds to the surface-solvent affinity. Note that, since χ_S is defined as a vector product, it may be negative if the vectors $\left(\vec{\delta_P} - \vec{\delta_S}\right)$ and $\left(\vec{\delta_N} - \vec{\delta_S}\right)$ make an angle larger than 90° in the 3D Hansen space. It follows that the higher adsorption measured for PDMA than for PAAm may actually originate in the fact that PAAm is better solvated by water than PDMA. For P(DMA-AAm) copolymer chains (PAD samples), monomers are in competition for adsorption. From Figure 4, it is difficult to assess whether the variation of the adsorbed amount varies linearly with the copolymer composition. Actually, the theory does not predict this variation to be linear,[57,58] and past experiments indeed show that the variation can be quite strongly non-linear.[59,60]

Reinforcement in the linear regime, i.e. the dramatic enhancement of the elastic modulus of elastomers and gels in the presence of silica nanoparticles and of polymer-particle interactions, has been interpreted in various ways.[61–63] In filled elastomers, a key role was attributed to the presence of a rigid polymer layer in the vicinity of the particle surfaces.[52,64] A network of so-called glassy bridges may then be formed, which leads to reinforcement effects far beyond those expected from hydrodynamic effects typically described by the Guth and Gold and further similar models. Besides, this interpretation accounts for the strong temperature variation of reinforcement within a wide temperature range above the T_g of the elastomer matrix.[65] In hybrid gels the situation is of course largely different, as the overall mobility of the matrix (polymer plus solvent) precludes the formation of a nanometric rigid layer. The local mobility of the polymer in the vicinity of the particles however plays a

major role, as it is affected by the presence of strong adsorption of polymer chains on the particles. One possible interpretation would be that the strong enhancement of the modulus may be explained through a corresponding strong increase of the apparent crosslink density in the presence of particles, adsorption points at the surface of the silica particles acting as additional effective crosslinks.

This hypothesis was checked by characterizing the apparent crosslink density by DQ proton NMR measurements. It was shown that the apparent crosslink density is enhanced by a factor of about two in the presence of silica NPs (Figure 11), while the modulus increases by a factor about 5 as compared to the Guth and Gold prediction given by equation 2 and reported in Figure 16.

On the other hand, the macroscopic nominal strain determined from stress-strain curves significantly underestimates the local strain in the gel matrix itself[66]. It was shown that the strain amplification factor X can be estimated as[67]:

$$X = \frac{1}{1 - \Phi} \tag{3}$$

with Φ the silica volume fraction. For PDMA hybrid gel (NC_D), equation 3 gives $X = 1.26$ for $\Phi_{Si} = 0.2$, meaning that the local strain at failure would reach approximatively 1000% within the PDMA gel (see Figure 15). Conversely, PAAm hybrid gels (NC_A) show quasi linear stress-strain curves with much lower strain and stress at break, of the order of the corresponding chemical gels. The strain at failure of the NC_A gel would be about 380 % (for a nominal strain at failure of about 300%, see Figure 15).

5 Conclusion

Polymer-particle interactions were tuned in model hybrid hydrogels by changing the chemical nature of the gel network from PDMA, which adsorbs on silica in aqueous solution, to PAAm, which does not, while maintaining very similar dispersion states of the nanoparticles. A

high pH value was used alternatively to inhibit PDMA adsorption by changing the silica surface chemistry. These experiments were designed to selectively investigate the impact of polymer adsorption on the behavior of hybrid gels, by maintaining constant other parameters which affect the properties, such as the homogeneity of the gels and the dispersion state of nanoparticles.

Compared to PDMA networks, the use of PAAm as the main component of the polymer matrix induces a significant weakening of the mechanical behavior of the hybrid gels. A strong decrease of the stiffness, of the dissipative properties and of the toughness are observed.

All these results emphasize the key role played by polymer adsorption on silica as the main reinforcement mechanism for hybrid gels with well-dispersed silica nanoparticles.

Tuning the adsorption enables tuning the modulus in the linear regime up to far above the hydrodynamic prediction. Besides, strong adsorption not only provides strong reinforcement in terms of stiffness, it also considerably increases the energy at break (the integral of the stress-strain curve) and the toughness (fracture energy). One key aspect to consider is the dissipation ability of the material provided by dynamic exchange at the polymer-silica surface, which may enable relaxing local stress concentration.

6 Acknowledgements

We thank D. Hourdet (Sciences et Ingénierie de la Matière Molle, ESPCI Paris) for fruitful discussions.

7 Supplementary information

- Synthesis of PDMA, PAAm and P(AAm-co-DMA) polymer chains by ATRP
- Experimental procedures

- Low-field ^{1}H time-domain NMR measurements
- Analysis of SAXS measurements in hybrid gels

References

(1) Haraguchi, T., K.; Takehisa Nanocomposite hydrogels: A Unique Organic-Inorganic network Structure with Extraordinary Mechanical, Optical ans Swelling/Deswelling Properties. *Advanced Materials* **2002**, *14*, 1120–1124.

(2) Suzuki, T.; Endo, H.; Osaka, N.; Shibayama, M. Dynamics and microstructure analysis of N-isopropylacrylamide/silica hybrid gels. *Langmuir* **2009**, *25*, 8824–8832.

(3) Fukasawa, M.; Sakai, T.; Chung, U. I.; Haraguchi, K. Synthesis and Mechanical Properties of a Nanocomposite Gel Consisting of a Tetra-PEG/Clay Network. *Macromolecules* **2010**, *43*, 4370–4378.

(4) Haraguchi, K.; Li, H. J.; Ren, H.; Zhu, M. Modification of Nancomposite Gels by Irreversible Rearrangement of Polymer/Clay Network Structure through Drying. *Macromolecules* **2010**, *43*, 9848–9853.

(5) Li, H. J.; Jiang, H.; Haraguchi, K. Ultrastiff, Thermoresponsive Nanocomposite Hydrogels Composed of Ternary Polymer–Clay–Silica Networks. *Macromolecules* **2018**, *51*, 529–539.

(6) Lafuma, F.; Wong, K.; Cabane, B. Bridging of Colloidal Particles through Adsorbed Polymers. *Journal of Colloid and Interface Science* **1991**, *143*, 9–21.

(7) Rose, S.; Dizeux, T., A.and Narita; Hourdet, D.; Marcellan, A. Time Dependence of Dissipative and Recovery Processes in Nanohybrid Hydrogels. *Macromolecules* **2013**, *46*, 4095–4104.

(8) Rose, S.; Marcellan, A.; Hourdet, D.; Creton, C.; Narita, T. Dynamics of Hybrid Polyacrylamide Hydrogels Containing Silica Nanoparticles Studied by Dynamic Light Scattering. *Macromolecules* **2013**, *53*, 4567–4574.

(9) Rose, S.; Marcellan, A.; Narita, T.; Boue, F.; Cousin, F.; Hourdet, D. Structure investigation of nanohybrid PDMA/silica hydrogels at rest and under uniaxial deformation. *Soft Matter* **2015**, *11*, 5905–5917.

(10) Haraguchi, K.; Li, H. J. Control of the coil-to-globule transition and ultrahigh mechanical properties of PNIPA in nanocomposite hydrogels. *Angew Chem Int Ed Engl* **2005**, *40*, 6500–6504.

(11) Rose, S.; Prevoteau, A.; Elziere, D., P.and Hourdet; Marcellan, A.; Leibler, L. Nanoparticle solutions as adhesives for gels and biological tissues. *Nature* **2014**, *505*, 382–385.

(12) Lin, W. C.; Fan, W.; Marcellan, A.; Hourdet, D.; Creton, C. Large Strain and Fracture Properties of Poly(dimethylacrylamide)/Silica Hybrid Hydrogels. *Macromolecules* **2010**, *43*, 2554–2563.

(13) Lin, W. C.; Marcellan, A.; Hourdet, D.; Creton, C. Effect of polymer–particle interaction on the fracture toughness of silica filled hydrogels. *Soft Matter* **2011**, *7*, 6578–6582.

(14) Ye, L.; Tang, Y.; Qiu, D. Enhance the mechanical performance of polyacrylamide hydrogel by aluminium-modified colloidal silica. *Colloids and Surfaces A: Physicochemical and Engineering Aspects* **2014**, *447*, 103–110.

(15) Jang, J.; Park, H. Formation and structure of polyacrylamide-silica nanocomposites by sol-gel process. *Journal of Applied Polymer Science* **2002**, *83*, 1817–1823.

(16) Petit, L. Responsive hybrid self-assemblies in aqueous media. *Langmuir* **2007**, *23*, 147–158.

(17) Griot, O.; Kitchener, J. A. Role of Surface Silanol Groups in the Flocculation of Silica Suspensions by Polyacrylamide Part 1 .Chemistry of the Adsorption Process. *Transactions of the Faraday Society* **1965**, *61*, 1026–1031.

(18) Bessaies-Bey, H.; Fusier, J.; Harrisson, S.; Destarac, M.; Jouenne, S.; Passade-Boupat, N.; Lequeux, F.; d'Espinose de Lacaillerie, J. B.; Sanson, N. Impact of polyacrylamide adsorption on flow through porous siliceous materials: State of the art, discussion and industrial concern. *Journal of Colloid and Interface Science* **2018**, *531*, 693–704.

(19) Silberberg, A. Adsorption of Flexible Macromolecules. IV. Effect of Solvent-Solute Interactions, Solute Concentration, and Molecular Weight. *J. Chem. Phys.* **1968**, *48*, 2835–2851.

(20) Semenov, A. N.; Bonet-Avalos, J.; Johner, A.; Joanny, J. F. Adsorption of Polymer Solutions onto a Flat Surface. *Macromolecules* **1996**, *29*, 2179–2196.

(21) Molinari, N.; Angioletti-Uberti, S. Nanoparticle Organization Controls Their Potency as Universal Glues for Gels. *Nano Lett* **2018**, *18*, 3530–3537.

(22) Carlsson, L.; Rose, S.; Hourdet, D.; Marcellan, A. Nano-hybrid self-crosslinked PDMA/silica hydrogels. *Soft Matter* **2010**, *6*, 3619–3631.

(23) Shapiro, Y. E. Structure and dynamics of hydrogels and organogels: An NMR spectroscopy approach. *Progress in Polymer Science* **2011**, *36*, 1184–1253.

(24) Lange, F.; Schwenke, K.; Kurakazu, M.; Akagi, Y.; Chung, U.-I.; Lang, M.; Sommer, J.-U.; Sakai, T.; Saalwächter, K. Connectivity and Structural Defects in Model Hydrogels: A Combined Proton NMR and Monte Carlo Simulation Study. *Macromolecules* **2011**, *44*, 9666–9674.

(25) Hoepfner, J.; Guthausen, G.; Saalwächter, K.; Wilhelm, M. Network Structure and Inhomogeneities of Model and Commercial Polyelectrolyte Hydrogels as Investigated by Low-Field Proton NMR Techniques. *Macromolecules* **2014**, *47*, 4251–4265.

(26) Es Sayed, J.; Lorthioir, C.; Perrin, P.; ; Sanson, N. PEGylated NiPAM microgels: synthesis, characterization and colloidal stability. *Soft Matter* **2019**, *15*, 963–972.

(27) Ihlenburg, R. B. J.; Mai, T.; Thunemann, A. F.; Baerenwald, R.; Saalwächter, K.; Koetz, J.; Taubert, A. Sulfobetaine Hydrogels with a Complex Multilength-Scale Hierarchical Structure. *Journal of Physical Chemistry B* **2021**, *125*, 3398–3408.

(28) Destarac, M. Controlled Radical Polymerization: Industrial Stakes, Obstacles and Achievements. *Macromolecular Reaction Engineering* **2010**, *4*, 165–179.

(29) Donovan, M. S.; Sanford, T. A.; Lowe, A. B.; Sumerlin, B. S.; Mitsukami, Y.; McCormick, C. L. RAFT Polymerization of N,N-Dimethylacrylamide in Water. *Macromolecules* **2002**, *35*, 4570–4572.

(30) Baum, M.; Brittain, W. Synthesis of Polymer Brushes on Silicate Substrates via Reversible Addition Fragmentation Chain Transfer Technique. *Macromolecules* **2002**, *35*, 610–615.

(31) Lutz, J.; Matyjaszewski, K. Stereoblock Copolymers and Tacticity Control in Controlled/Living Radical Polymerization. *J. Am. Chem. Soc.* **2003**, *125*, 6986–6993.

(32) Xia, J.; Matyjaszewski, K. Atom Transfer Radical Polymerization. *Chem. Rev.* **2002**, *101*, 2921–2990.

(33) Read, E.; Guinaudeau, A.; Wilson, D. J.; Cadix, A.; Violleau, F.; Destarac, M. Low temperature RAFT/MADIX gel polymerisation: access to controlled ultra-high molar mass polyacrylamides. *Polymer Chemistry* **2014**, *25*, 2202–2207.

(34) Ding, S.; Radosz, M.; Shen, Y. Atom Transfer Radical Polymerization of N,N-Dimethylacrylamide. *Macromol. Rapid. Comm.* **2004**, *25*, 632–636.

(35) Wever, D. A. Z.; Raffa, P.; Picchioni, F.; Broekhuis, A. A. Acrylamide Homopolymers and Acrylamide–N-Isopropylacrylamide Block Copolymers by Atomic Transfer Radical Polymerization in Water. *Macromolecules* **2012**, *45*, 4040–4045.

(36) Fechete, R.; Demco, D. E.; Blümich, B. Chain orientation and slow dynamics in elastomers by mixed magic-Hahn echo decays. *J. Chem. Phys.* **2003**, *118*, 2411–2421.

(37) Papon, A.; Saalwächter, K.; Schäler, K.; Guy, L.; Lequeux, F.; Montes, H. Low-Field NMR Investigations of Nanocomposites: Polymer Dynamics and Network Effects. *Macromolecules* **2011**, *44*, 913–922.

(38) Saalwächter, K.; Ziegler, P.; Spyckerelle, O.; Haidar, B.; Vidal, A.; Sommer, J.-U. 1H multiple-quantum nuclear magnetic resonance investigations of molecular order distributions in poly(dimethylsiloxane) networks: Evidence for a linear mixing law in bimodal systems. *Journal of Chemical Physics* **2003**, *119*, 3468–3482.

(39) Saalwächter, K. Proton multiple-quantum NMR for the study of chain dynamics and structural constraints in polymeric soft materials. *Progress in Nuclear Magnetic Resonance Spectroscopy* **2007**, *51*, 1–35.

(40) Frantz, P.; Granick, S. Exchange-Kinetics of Adsorbed Polymer and the Achievement of Conformational Equilibrium. *Macromolecules* **1994**, *27*, 2553–2558.

(41) Chaplain, V.; Janex, M. L.; Lafuma, F.; Graillat, C.; Audebert, R. Coupling between polymer adsorption and colloidal particle aggregation. *Colloid Polym Sci* **1995**, *273*, 984–993.

(42) Hourdet, D.; Petit, L. Hybrid Hydrogels: Macromolecular Assemblies through Inorganic Cross-Linkers. *Macromolecular Symposia* **2010**, *291-292*, 144–158.

(43) Scheutjens, J.; Fleer, G. J. Statistical theory of the adsorption of interacting chain molecules. 1. Partition function, segment density distribution, and adsorption isotherms. *J. Phys. Chem.* **1979**, *83*, 1619–1635.

(44) Van der beek, G. P.; Cohen-Stuart, M. A. Polymer Adsorption and Desorption Studies via 1H NMR Relaxation of the Solvent. *Langmuir* **1991**, *7*, 327–334.

(45) Nelson, A.; Jack, K. S.; Cosgrove, T.; Kozak, D. NMR Solvent Relaxation in Studies of Multicomponent Polymer Adsorption. *Langmuir* **2002**, *18*, 2750–2755.

(46) Cooper, C. L.; Cosgrove, T.; van Duijneveldt, J. S.; Murray, M. Competition between Polymers for Adsorption on Silica: A Solvent relaxation NMR and Small-Angle Neutron Scattering Study. *Langmuir* **2013**, *29*, 12670–12678.

(47) Valentín, J. L.; Mora-Barrantes, I.; Carretero-González, J.; López-Manchado, M. A.; Sotta, P.; Long, D. R.; Saalwächter, K. Novel Experimental Approach To Evaluate Filler-Elastomer Interactions. *Macromolecules* **2010**, *43*, 334–346.

(48) Vieyres, A.; Pérez-Aparicio, R.; Albouy, P.-A.; Sanseau, O.; Saalwächter, K.; Long, D. R. R.; Sotta, P. Sulfur-Cured Natural Rubber Elastomer Networks: Correlating Cross-Link Density, Chain Orientation, and Mechanical Response by Combined Techniques. *Macromolecules* **2013**, *46*, 889–899.

(49) Lang, M.; Sommer, J.-U. Analysis of Entanglement Length and Segmental Order Parameter in Polymer Networks. *Phys. Rev. Lett.* **2010**, *104*, 177801.

(50) Guth, E. Theory of filler reinforcement. *Journal of Applied Physics* **1945**, *16*, 20–25.

(51) Guth, E.; Simha, R. Explorations of the viscosity of suspensions and solutions 3. The viscosity of sphere suspensions (The calculation of wall influence and the exchange effect in viscosity as well as in rotating spheres). *Kolloid-Zeitschrift* **1936**, *74*, 266–275.

(52) Berriot, J.; Montes, H.; Lequeux, F.; , D., Long; Sotta, P. Evidence for the Shift of the Glass Transition near the Particles in Silica-Filled Elastomers. *Macromolecules* **2002**, *35*, 9756–9762.

(53) Lake, G. J.; Thomas, A. G. The Strength of Highly Elastic Materials. *Proceedings of the Royal Society London* **1967**, *300*, 108–119.

(54) Gent, A. N. *Engineering with rubbers. How to design rubber components*; Hanser, 2000.

(55) Appel, E. A.; Scherman, O. A. Gluing gels: A nanoparticle solution. *Nat Mater* **2014**, *13*, 231–232.

(56) Laurens, J.; Jolly, J.; Ovarlez, G.; Fay, H.; Chaussée, T.; Sotta, P. Competitive Adsorption between a Polymer and Solvents onto Silica. *Langmuir* **2020**, *36*, 7669–7680.

(57) Marques, C. M.; Joanny, J. F. Adsorption of Random Copolymers. *Macromolecules* **1990**, *23*, 268–276.

(58) Fleer, G. J.; Cohen-Stuart, M. A.; Scheutjens, J. M. H. M.; Cosgrove, T.; Vincent, B. *Polymers at Interfaces*; Chapman & Hall, 1993.

(59) Kawaguchi, M.; Inoue, A.; Takahashi, A. Adsorption of Ethylene-Vinyl Acetate Co-Polymer on Silica Surface. *Polymer Journal* **1983**, *15*, 537–542.

(60) Kobayashi, K.; Araki, K.; Imamura, Y.; Endo, R. ESR Studies of the Adsorption Behavior of Styrene-Methyl Metacrylate Copolymer at the Solid-Liquid Interface. *Bulletin of the Chemical Society of Japan* **1990**, *63*, 511–515.

(61) Wang, M. J. Effect of Polymer Filler and Filler-Filler Interactions on Dynamic Properties of Filled Vulcanizates. *Rubber Chemistry and Technology* **1998**, *71*, 520–589.

(62) Heinrich, G.; Klüppel, M. Recent Advances in the Theory of Filler Networking in Elastomers. *Filled Elastomers Drug Delivery Systems* **2002**, *160*, 1–44.

(63) Mujtaba, A.; Keller, M.; Ilisch, S.; Radusch, H.; Thurn-Albrecht, T.; Saalwachter, K.; Beiner, M. Mechanical Properties and Cross-Link Density of Styrene–Butadiene Model Composites Containing Fillers with Bimodal Particle Size Distribution. *Macromolecules* **2012**, *45*, 6504–6515.

(64) Berriot, J.; Lequeux, F.; Monnerie, L.; Montes, H.; Long, D.; Sotta, P. Filler-Elastomer Interaction in Model Filled Rubbers, a 1H NMR Study. *J. Non-Cryst. Solids* **2003**, *307*, 719–724.

(65) Merabia, S.; Sotta, P.; Long, D. R. A Microscopic Model for the Reinforcement and the Nonlinear Behavior of Filled Elastomers and Thermoplastic Elastomers (Payne and Mullins Effects). *Macromolecules* **2008**, *41*, 8252–8266.

(66) Mullins, L.; Tobin, N. R. Theoretical Model for the Elastic Behavior of Filler-Reinforced Vulcanized Rubbers. *Rubber Chemistry and Technology* **1957**, *30*, 555–571.

(67) Domurath, J.; Saphiannikova, M.; Ausias, G.; Heinrich, G. Modelling of stress and strain amplification effects in filled polymer melts. *J. of Non-Newtonian Fluid Mechanics* **2012**, *171-172*, 8–16.